Progress in nano-biocomposites based on polysaccharides and nanoclays

Frédéric Chivrac, Eric Pollet, Luc Avérous *

LIPHT-ECPM, Université de Strasbourg, 25 rue Becquerel, 67087 Strasbourg Cedex 2, France

ARTICLE INFO

ABSTRACT

The last decade has seen the development of an alternative chemistry, which intends to reduce the human impact on the environment. The polymers are obviously involved into this tendency and numerous bio-sourced plastics (bioplastics), such as polylactide, plasticized starch, etc., have been elaborated. However, even if a lot of commercial products are now available, their properties (mechanical properties, moisture sensitivity) have to be enhanced to be really competitive with the petroleum-based plastics. One of the most promising answers to overcome these weaknesses is the elaboration of nano-biocomposites, namely the dispersion of nano-sized filler into a biopolymer matrix. This review reports the last developments in nano-biocomposites based on polysaccharides and nanoclays. The main elaboration strategies developed in starch, chitosan, cellulose acetate and pectin based nano-biocomposites elaborated with montmorillonite as the nanofiller are exposed herein. The corresponding dispersion state and properties are discussed.

© 2009 Elsevier B.V. All rights reserved.

Contents

* Corresponding author. Tel.: +33 3 68 852 784; fax: +33 3 68 852 716.
  E-mail address: luc.averous@unistra.fr (L. Avérous).

1. Introduction

As a result of the increasing awareness concerning the human impact on the environment and the constant increase in the fossil resources price, the last decade has seen the development of efficient solutions to produce new environmentally friendly materials. Particular attention has been paid to the replacement of conventional petroleum-based plastics by materials based on biopolymers, such as biodegradable polyester [1–4], proteins [5–7] or polysaccharides [8–11].

Many biopolymer definitions exist and some of them are ambiguous, but it is now accepted that biopolymers are biodegradable materials capable of undergoing decomposition thanks to microorganisms and enzymatic degradation (ASTM standard D-5488-94d). Depending on the degradation conditions (aerobic vs. anaerobic) and the medium, the material is decomposed into water, inorganic compounds, carbon dioxide and/or methane, and biomass. The biopolymers can be classified in four different categories [8]:

 (i) Agro-polymers extracted from biomass, such as starch, cellulose, proteins, chitin, etc.
 (ii) Polymers obtained by microbial production, such as the polyhydroxyalkanoates (PHA).
(iii) Polymers conventionally and chemically synthesized and whose monomers are obtained from agro-resources, such as the polylactic acid (PLA).
(iv) Polymers whose monomers are obtained from fossil resources, such as poly(ε-caprolactone) (PCL), polyesteramide (PEA), poly(butylene succinate-co-adipate) (PBSA), poly(butylene adipate-co-terephthalate) (PBAT).

The biopolymers produced from renewable resources are an elegant and innovating answer to replace conventional petroleum-based products and fit with a real sustainable development approach. However, to obtain suitable and competitive materials, some of theirs properties have to be enhanced (lower brittleness, moisture sensitivity, etc.). Consequently, even if the potential of these bio-based materials have been pointed out, until now, they are not widely used to replace non-degradable plastics. The common approach to tune their behaviors consists in the elaboration of multiphase materials, e.g., blends [12–14] or composites [15–18].

A new class of composite materials based on the incorporation of nano-sized fillers (nanofillers) has been investigated [19–26]. Depending on the nanofiller, nanocomposites could exhibit drastic modifications in their properties, as improved mechanical and barrier properties, higher transparency [20,27–32], etc. Such properties enhancements rely both on the nanofiller geometry and on the nanofiller surface area. This area may attain 600–800 m^2/g when the nanofiller is homogeneously dispersed and exfoliated (for montmorillonite nanoclay). The different nanofillers can be classified depending on their aspect ratio and geometry, such as (i) layered particles (e.g., clay), (ii) spherical (e.g., silica) or (iii) acicular ones (e.g., whiskers, carbon nanotubes). At present, the most intensive researches are focused on layered silicates, such as montmorillonite (MMT), due to their availability, versatility and respectability towards the environment and health. A wide range of nano-biocomposites (nanocomposites based on biopolymers) [33] have been elaborated with different matrices, such as, PCL [28,34–38], PLA [39–44] or PHA [45–47] or with agro-polymers [48–51], such as starch or chitosan and have demonstrated that nano-biocomposites elaboration could be a powerful strategy to overcome the conventional drawbacks of agro-based polymers.

The following paper presents an overview of the major recent developments in polysaccharides nano-biocomposites based on nanoclays. The main biopolymers, clays and nano-biocomposites elaboration processes will be discussed. The major systems will be extensively described and compared.

2. From the nanoclay to the nanocomposite

The following section will be focused on nanoclays, and more especially on phyllosilicate nano-particles, and on the nanocomposites elaboration protocols.

2.1. Phyllosilicates: structure, properties and organo-modification

Phyllosilicates are a wide family in which clays with different structure, texture or morphology can be found. For instance, the montmorillonite and the synthetic laponite clay are anisotropic particles with a thickness of one nanometer but a width of hundreds and tens nanometers, respectively.

2.1.1. Multi-scale structure

The phyllosilicates mainly present three organization levels depending on the observation scale, (i) the layer, (ii) the primary particle and (iii) the aggregate (Fig. 1).

 (i) The layer is equivalent to a disc or a platelet having a width varying from 10 nm to 1 μm and a thickness of 1 nm. These layers, and more especially the widest, are flexible and deformable.
 (ii) The primary particle is composed of five to ten stacked platelets. The cohesion of the structure is assured by Van der Waals and electrostatic attraction forces between the cations and the platelets. The stacking of these particles is perpendicular to the z direction and is disordered in the plan (x, y). The structure thickness is around 10 nm.
(iii) The aggregate is the association of primary particles orientated in all the directions. The size of the aggregates varies from 0.1 to 10 μm.

2.1.2. Nanoclays structure

The phyllosilicate crystal structure is based on the pyrophyllite structure $Si_4Al_2O_{10}(OH)_2$ and can be described as a crystalline 2:1 layered clay mineral with a central alumina octahedral sheet sandwiched between two silica tetrahedral sheets corresponding to seven atomic layers superposed (Fig. 2) [52]. This structure becomes $(Si_8)(Al_{4-y}Mg_y)O_{20}(OH)_4, M_y^+$ for the montmorillonite or $(Si_8)(Al_{6-y}Li_y)O_{20}(OH)_4, M_y^+$ for the hectorite. These differentiations are mainly due to the isomorphic substitutions that take place inside the aluminum oxide layer [53]. These substitutions induce a negative charge inside the clay platelet, which is naturally counter balanced by inorganic cations (Li^+, Na^+, Ca^{2+}, K^+, Mg^{2+}, etc.) located into the inter-layer spacing, The global charge varies depending on the phyllosilicates. For the smectite and the mica families, this charge varies from 0.4 to 1.2 and from 2 to 4 per unit cell, respectively (Table 1). The charge amount is characterized by the cationic exchange capacity (CEC) and corresponds to the amount of monovalent cations necessary to compensate the platelets negative charge, which is usually given in milliequivalent per 100 g (meq/100 g). For instance, the montmorillonite CEC
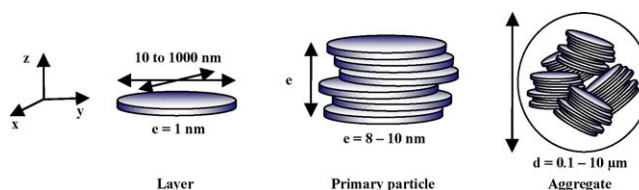

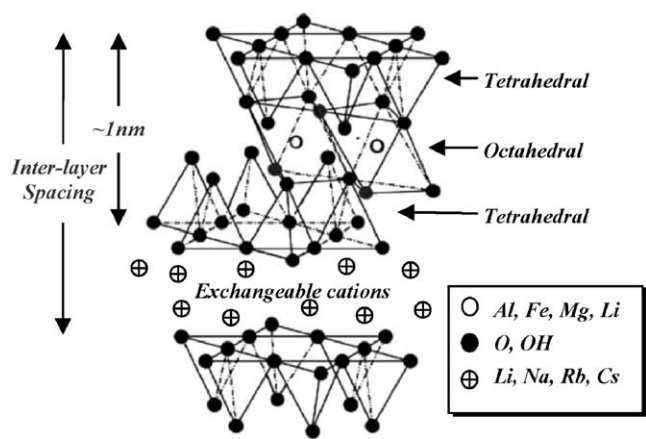**Fig. 1.** Phyllosilicate multi-scale structure.

Fig. 2. Structure of 2:1 phyllosilicates.

varies from 70 to 120 meq/100 g depending on their extraction site [54].

The distance observed between two platelets of the primary particle, named inter-layer spacing or d-spacing (d_{001}), depends on the silicate type. This value does not entirely depend on the layer crystal structure, but also on the type of the counter-cation and on the hydration state of the silicate. For instance, $d_{001} = 0.96$ nm for anhydrous montmorillonite with sodium as counter ion, but $d_{001} = 1.2$ nm in usual conditions. This increase is linked to the adsorption of one layer of water molecules between the clay platelets [19].

2.1.3. Phyllosilicate swelling properties

The phyllosilicate multi-scale structure has different porosity levels, which drive its swelling properties. The water absorption occurs thanks to the intercalated cation hydration, which lowers the attractive forces between the clay layers [55], and also thanks to the water capillarity phenomena, which take place into the inter-particle and inter-aggregate porosities [56,57]. For a given pressure, this swelling is characterized by a d_{001} increase until an equilibrium distance [58]. In general, the smaller is the cation and the lower is its charge, the higher the clay swelling is. For MMT, the swelling decreases depending on the cation chemical type according to the following trend: $Li^+ > Na^+ > Ca^{2+} > Fe^{2+} > K^+$ [59–61]. The potassium cation is a specific case because its size is equal to the dimension of the platelet surface cavity. Thus, the potassium is trapped into these cavities, leading to a lowering of its hydration ability.

2.1.4. Phyllosilicate organo-modification

To enhance the intercalation/exfoliation process into a polymer matrix, a chemical modification of the clay surface, with the aim to match the polymer polarity, is often carried out [19,20]. The cationic exchange is the most common technique, but other original techniques as the organosilane grafting [62,63], the use of ionomers [64,65] or block copolymers adsorption [66] are also used.

The cationic exchange consists in the inorganic cations substitution by organic ones. These cations are often alkylammonium surfactants having at least one long alkyl chain. Phosphonium salts are also interesting clay modifiers, thanks to their higher thermal stability, but they are not often used [67]. The ionic substitution is performed into water because of the clay swelling, which facilitates the organic cations insertion between the platelets. Then, the solution is filtered, washed with distilled water (to remove the salt formed during the surfactant adsorption and the surfactant excess) and lyophilized to obtain the organo-modified clay. In addition to the modification of the clay surface polarity, organo-modification increases the d_{001}, which will also further facilitate the polymer chains intercalation [68]. Various commercially available organo-modified montmorillonites (OMMT), which mainly differ from the nature of their counter-cation and their CEC, are produced with this technique (e.g., Cloisite® 15A, 20A, 30B... or Nanofil® 804...).

2.2. Nanocomposites elaboration protocol

The nanofiller incorporation into the polymer matrix can be carried out with three main techniques [19], (i) the in situ polymerization, (ii) the solvent intercalation or (iii) the melt intercalation process.

Depending on the process conditions and on the polymer/nanofiller affinity, different morphologies can be obtained. These morphologies can be divided in three distinct main categories, (i) microcomposites, (ii) intercalated nanocomposites or (iii) exfoliated nanocomposites [19–21]. For microcomposites, the polymer chains have not penetrated into the inter-layer spacing and the clay particles are aggregated. In this case, the designation as nanocomposite is abusive. In the intercalated structures, the polymer chains have diffused between the platelets leading to a d_{001} increase. In the exfoliated state, the clay layers are individually delaminated and homogeneously dispersed into the polymer matrix. Intermediate dispersion states are often observed, such as intercalated–exfoliated structures. This classification does not take into account the dispersion multi-scale structure, such as percolation phenomenon, preferential orientation of the clay layers, etc. [20].

2.2.1. In situ polymerization process

In this method, layered silicates are swollen into a monomer solution. Then, the monomer polymerization is initiated and propagated. The macromolecules molecular weight increases, leading to a d_{001} increase and sometimes to an almost fully exfoliated morphology for some studied systems [20]. However, since polysaccharides chains are synthesized during the plant growth and then extracted from the vegetal, this technique cannot be used to prepare polysaccharides nano-biocomposites.

2.2.2. Solvent intercalation process

This elaboration process is based on a solvent system in which the polymer is soluble and the silicate layers are swellable. The polymer is first dissolved in an appropriate solvent. In parallel, the

Table 1
Classification of 2:1 phyllosilicates.

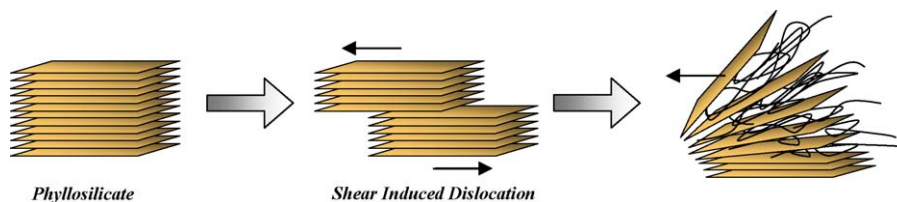| Charge per unit cell	Di-octahedral phyllosilicate	Tri-octahedral phyllosilicate
Smectites		
0.4–1.2	Montmorillonite $(Si_8)(Al_{4-y}Mg_y)O_{20}(OH)_4, M_x^+$	Hectorite $(Si_8)(Al_{6-y}Li_y)O_{20}(OH)_4, M_y^+$
	Beidellite $(Si_{8-x}Al_x)Al_4O_{20}(OH)_4, M_x^+$	Saponite $(Si_{8-x}Al_x)(Mg_6)O_{20}(OH)_4, M_x^+$
1.2–1.8	Illites $(Si_{8-x}Al_x)(Al_{4-y}M_y^{2+}O_{20}(OH)_4, K_{x+y}^+$	Vermiculite $(Si_{8-x}Al_x)(Mg_{6-y}M_y^{3+})O_{20}(OH)_4, K_{x+y}^+$
Micas		
2	Muscovite $(Si_6Al_2)(Al_4)O_{20}(OH)_2, K_2^+$	Phlogopites $(Si_6Al_2)(Mg_6)O_{20}(OH)_2, K_2^+$
4	Margarite $(Si_4Al_4)(Al_4)O_{20}(OH)_2, Ca_2^{2+}$	Clintonite $(Si_4Al_4)(Mg_6)O_{20}(OH)_2, Ca_2^{2+}$

Fig. 3. Mechanism leading to clay exfoliation under shearing [70].

clay (organo-modified or not) is swollen and dispersed into the same solvent or another one to obtain a miscible solution. Both systems are pooled together leading to a polymer chains intercalation. Then, the solvent is evaporated to obtain nanocomposite materials. Nevertheless, for non water-soluble polymers, this process involves the use of large amount of organic solvents, which is environmentally unfriendly and cost prohibitive. Moreover, a small amount of solvent may remain in the final product at the polymer/clay interface creating lower interfacial interaction between the polymer and the clay surfaces [69]. Thus, this technique is mainly used in academic studies. Since some polysaccharides, such as chitosan or pectin, cannot be melt processed due to high thermal or thermo-mechanical degradations, the solvent process has been extensively used to produce polysaccharide/clay hybrid materials.

2.2.3. Melt intercalation process

Both the polymer and the clay are introduced simultaneously into a melt mixing device (extruder, internal mixer, etc.). According to Dennis et al. [70], in addition to the polymer/nanofiller affinity, two main process parameters favor the nano-dispersion of the nanoclay. These parameters, which are the driving force of the intercalation-exfoliation process into the matrix, are (i) the residence time and (ii) the shearing. The shearing is necessary to induce the platelets delamination from the clay tactoïds. The extended residence time is needed to allow the polymer chains diffusion into the inter-layer gallery and then to obtain an exfoliated morphology (Fig. 3).

This simple process has extensively been used to prepare polysaccharide nano-biocomposite materials. Nevertheless, the thermal or thermo-mechanical inputs lead to partial chains degradation. Moreover, the high residence times needed to enhance the clay exfoliation process favor the matrix degradation. Therefore, it is necessary to balance the process parameters to minimize the chains degradation and to obtain a well exfoliated morphology.

3. Polysaccharides-based nano-biocomposites

Polysaccharides are the most abundant macromolecules in the biosphere. These complex carbohydrates constituted of monosaccharides joined together by glycosidic bonds are often one of the main structural elements of plants and animals exoskeleton (e.g., cellulose, carrageenan, chitin, etc.) or have a key role in the plant energy storage (e.g., starch, paramylon, etc.).

The following chapter is focused on the main studied nano-biocomposite based on nanoclay and polysaccharides, namely starch and its derivatives, cellulose, chitosan and pectin. Throughout this paper, the nanofillers used to produce nano-hybrid materials are designated according to the abbreviations given in Table 2.

3.1. Starch

Starch is mainly extracted from cereals (wheat, corn, rice, etc.) and from tubers (potatoes, manioc, etc.). It is stocked into seeds or roots and represents the main plant energy reserve.
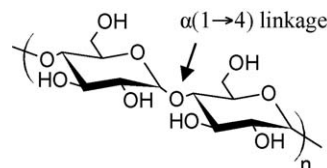

Fig. 4. Amylose chemical structure.

3.1.1. Native starch structure

Depending on the botanical origin of the plant, starch granules can have very different shapes (sphere, platelet, polygon, etc.) and size (from 0.5 to 175 μm). These granules are composed of two α-D-glucopyranose homopolymers, the amylose and the amylopectin. Their proportions into the granules depend directly on the botanical source [71]. In addition, starch also contains, in smaller proportion, other compounds such as proteins, lipids and minerals (Table 3). The amylose is mainly a linear polysaccharide composed of D-glucose units linked by $\alpha(1 \rightarrow 4)$ linkages (Fig. 4). These chains are partially ramified with some $\alpha(1 \rightarrow 6)$ linkages. Depending on the botanical source and the extraction process, the amylose molecular weight varies from 10^5 to 10^6 g mol^{-1} with a polydispersity ranging from 1.3 to 2.1 [72–74]. The amylose chains show a single or double helix conformation with a rotation on the $\alpha(1 \rightarrow 4)$ linkage [75].

The amylopectin is the main starch component and has the same monomeric unit as amylose. It shows 95% of $\alpha(1 \rightarrow 4)$ and 5% of $\alpha(1 \rightarrow 6)$ linkages. These latter are found every 24–79 glucose units [76] and bring to the amylopectin a highly branched structure. Consequently, the amylopectin structure and organization can be seen as a grape with pending chains (Fig. 5) [77].

The starch granule organization consists in an alternation of crystalline and amorphous areas leading to a concentric structure [78]. The amorphous areas are constituted of the amylose chains and the amylopectin branching points. The semi-crystalline areas are mainly composed of the amylopectin side chains. Some co-crystalline structures with the amylose chains have been also
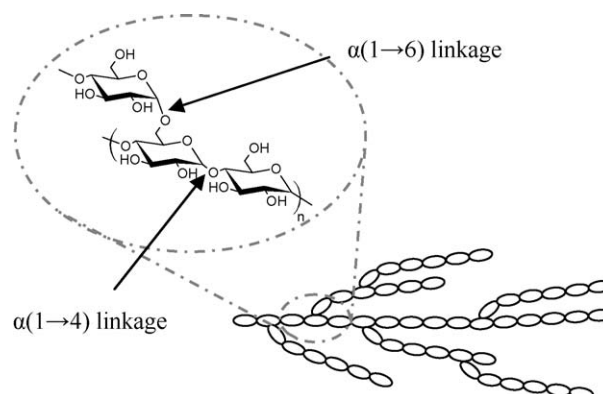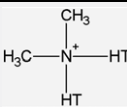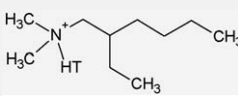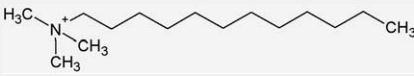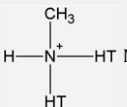

Fig. 5. Amylopectin chemical and grape structure [77].

Table 2
Nanofiller types (trade-name and code) and their corresponding counter-ion chemical structure.

Code	Name	Counter-Cation
MMT-Na	Natural sodium montmorillonite	
OMMT-Alk1	Cloisite® 15A, Southern Clay	Dimethyl-dihydrogenated tallow ammonium
OMMT-Alk2	Cloisite® 6A, Southern Clay	
OMMT-Alk3	Cloisite® 20A, Southern Clay	Dimethyl-hydrogenated tallow-2-ethylhexyl ammonium
OMMT-Alk4	Cloisite® 25A, Southern Clay	
OMMT-Alk5	Nanomer® I.30E, Nanocor	Octadecyl ammonium
OMMT-Alk6	/	Trimethyldodecyl ammonium
OMMT-Alk7	Cloisite® 93A, Southern Clay	Methyl-dihydrogenated tallow ternary ammonium hydrogen sulfate
OMMT-Bz	Cloisite® 10A, Southern Clay	Dimethyl-benzyl-hydrogenated tallow ammonium
OMMT-Bz2	Bentone® 111, Elementis Specialties	
OMMT-OH1	Cloisite® 30B, Southern Clay	Methyl-tallow-bis-2-hydroxyethyl ammonium
OMMT-OH2	Nanofil® 804, Süd Chemie	
OMMT-EtA	/	Ethanolamine
OMMT-CitA	/	Citric acid
OMMT-CS	/	Cationic starch

T = Tallow (∼65% C18; ∼30% C16; ∼5% C14), HT = Hydrogenated Tallow.

identified [79,80]. Four allomorphic starch structures exist [79]. Depending on the botanical origin, starch granules present a crystallinity varying from 20 to 45%.

3.1.2. Plasticized starch elaboration and properties

Because of the numerous inter-molecular hydrogen bonds existing between the chains, starch melting temperature is higher than its degradation temperature [81,82]. Consequently, to elaborate a plastic-like material it is necessary to introduce high water content or/and some unvolatile plasticizers (glycerol, sorbitol, etc.) which decrease the glass transition and the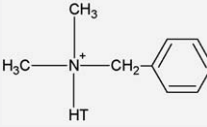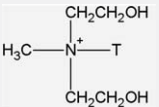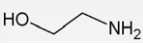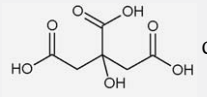 melting temperature [83,84]. These plasticized materials are currently named "thermoplastic starch" or "plasticized starch". To be transformed, the starch granule structure has to be disrupted. The disruption can be obtained either by solvent-casting process or by a melting process where starch and the plasticizers are mixed under thermo-mechanical treatment.

Solvent-assisted starch granules disruption is mostly carried out with water. At ambient temperature, starch remains insoluble in water and keeps its granular structure. Water temperature increase induces an irreversible swelling named "gelatinization". During this gelatinization, the amylose is rather solubilized, the granule semi-crystalline structure disappears and the granules swell rapidly. This phenomenon occurs at a given temperature

Table 3
Composition and physical chemical characteristics of different starches.

Starch	Amylose* (%)	Lipids* (%)	Proteins* (%)	Minerals* (%)	Crystallinity (%)	Water content† (%)
Wheat	26–27	0.63	0.30	0.10	36	13
Corn	26–28	0.63	0.30	0.10	39	12–13
Waxy Maize	<1	0.23	0.10	0.10	39	/
Amylocorn	52–80	1.11	0.50	0.20	19	/
Potato	20–24	0.03	0.05	0.30	25	18–19

* Dry-basis proportion.
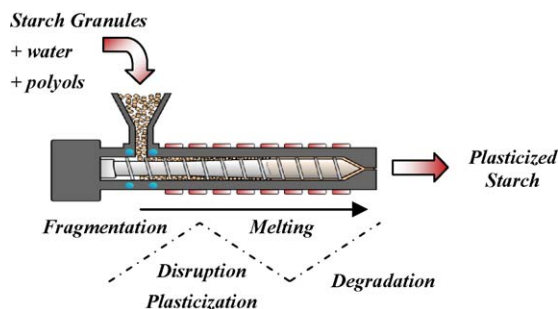† Water content after stabilization at 65%RH and 20 °C.

Fig. 6. Schematic representation of the starch extrusion process.

defined as "gelatinization temperature" (T_{gel}) which depends on the starch botanical origin [85–87]. To obtain a quite full starch solubilization hot DMSO is often used as solvent. Then, this solvent is volatilized under vacuum and heat.

The starch melting process is often carried out in association with plasticizers to obtain a homogeneous molten phase. During the thermo-mechanical process, e.g., extrusion, different and successive phenomena occur (Fig. 6) [8].

The starch granules disruption being dependent of the specific mechanical energy provided during the process, this material could be described as a "thermo-mechanical-plastic" material [88,89].

During the process, amylose and amylopectin degradation occurs and this phenomenon is obviously dependent on the thermal and mechanical energy brought to the system. Numerous studies were conducted to determine the degradation mechanism and to understand the contribution of each parameter [90–97].

Since starch is a hydrophilic material, water is the best plasticizer [84,98–100]. Nevertheless, the water content and thus the plasticized starch properties are strongly dependent on the storage conditions (temperature and atmosphere relative humidity). This drawback is partially solved with the use of less volatile plasticizers, which present lower plasticization efficiency. These compounds (polyols), bearing hydroxyl groups, can interact with the starch chains through hydrogen bonds. Glycerol is the most common plasticizer [101–104], but numerous other polyols, such as sorbitol [105], xylitol [106], fructose [107], glucose, [108] glycols [109], etc. or plasticizer with amino groups, like urea, can be used [109]. Nevertheless, these plasticizers are more hydrophilic than starch and are also sensitive to the relative humidity.

Depending on the plasticizer content, starch may display one or two relaxation, corresponding to a homogeneous or multiphasic material. Lourdin et al. [103,110] have demonstrated that a phase separation occurs for glycerol content higher than 27 wt% dry-basis. The corresponding second relaxation (named β) is consistent with the glycerol glass transition and occurs around −50 to −70 °C. This secondary transition is dependent on the glycerol concentration and more particularly on the 'free' glycerol [13,111]. The main relaxation (named α) is attributed to the plasticized starch T_g and

this temperature decreases when the glycerol content increases from 0 to 25 wt% [112].

Several studies were also performed in order to highlight the different interactions taking place in water/glycerol/starch multiphasic systems and to determine the influence of the water content at equilibrium [103,113]. The results have shown that the higher the water content, the lower the plasticized starch T_g.

The great influence of the water and glycerol content on the starch properties has also been highlighted by the "so-called" anti-plasticization effect [105,112]. Indeed, for glycerol concentration below 12 wt%, a remarkable behavior occurs since a decrease in the stress and the strain at break correlated to a rise in plasticizer content is observed. The same trend has also been evidenced in sorbitol plasticized systems and is assigned to the formation of a physical network stabilized by hydrogen bonds between the plasticizer and the starch chains, leading to a hardening of the material.

Plasticized starch mechanical properties also evolve with time due to molecular reorganization, which is dependent on the process protocol and the storage conditions. When the samples are stored below the T_g, the samples will undergo physical ageing with a material densification [114]. When $T > T_g$, the samples will retrograde with a crystallinity increase [115]. The physical ageing is observed for materials with plasticizer content lower than 25 wt% [82,116]. This phenomenon induces a hardening and a decrease of the strain at break. The retrogradation takes place after the amylose crystallization and concerns the amylopectin crystallization. This phenomenon is slow since it lasts for more than a month [13,117] and induces a strong variation of the mechanical properties [80,118–120]. Thus, even if these two phenomena are different, both of them induce internal stress into the material, which leads to an embrittlement characterized by a stiffness increase correlated to a strain at break decrease (Table 4).

The mechanical properties also strongly depend on the amylose/amylopectin ratio, which vary with the botanical origin. Amylopectin-rich starches are ductile [119] whereas those rich in amylose have higher modulus and lower strain at break [118].

3.1.3. Starch-based nano-biocomposites

Starch has been the most studied polysaccharide in nano-biocomposite systems, mainly into its plasticized state [49–51,121–147], but also with blends elaborated with PLA [148–151], PCL [152–159] or poly(vinyl alcohol) (PVAL) [146] or with chemically modified (e.g., acetylated) starch matrices [160,161].

3.1.3.1. Plasticized starch-based nano-biocomposites.
To reach exfoliation for plasticized starch-based nano-biocomposites, different nanofillers and elaboration protocols were developed. First, from 1 to 9 wt% of rather hydrophobic nanofillers were incorporated into starch plasticized with glycerol by melt blending [49,50, 123,125,126] (internal batch mixer or into a twin screw extruder) or solvent process [141]. It was clearly demonstrated that the incorporation of OMMT-Alk1 [123], OMMT-Alk2 [49] or OMMT-

Table 4
Wheat starch—tensile test parameters vs. storage time and glycerol content [13].

Ratio glycerol/starch	2 weeks of ageing			6 weeks of ageing		
	Young's modulus (MPa)	Stress at break (MPa)	Strain at break (%)	Young's modulus (MPa)	Stress at break (MPa)	Strain at break (%)
0.135	997 (59)	21.4 (1.0)	3.8 (0.3)	1,144 (42)	21.4 (1.7)	3.4 (0.4)
0.257	52 (9)	3.3 (0.1)	126.0 (2.0)	116 (11)	4.0 (0.1)	104.0 (4.7)
0.358	26 (4)	2.6 (0.1)	110.0 (11.1)	45 (5)	3.3 (0.1)	98.2 (5.2)
0.538	2 (1)	0.6 (0.2)	90.7 (4.8)	11 (1)	1.4 (0.1)	60.4 (5.2)

Samples stored at 23 °C and 50%RH.

Bz [49,123] led to the formation of conventional micro-biocomposites. This structure has been evidenced by the constant values of the basal d_{001} from X-ray diffraction experiments. Better results were obtained with OMMT-Alk5 [141] and OMMT-Alk7 [125], the corresponding nano-biocomposites displaying a slight shift in d_{001} towards lower angles. The dispersion of the more hydrophilic OMMT-OH1 led to higher dispersion state with a shift in the d_{001} value to lower angle and a strong decrease in the diffraction peak intensity [49,50,123,126]. This morphology was likely achieved thanks to the hydrogen bonds established between the hydroxyl groups brought by the carbohydrate chains and the clay surfactant [50].

Besides, nano-biocomposites based on plasticized starch with glycerol were elaborated with MMT-Na. Thanks to the hydrophilic nature of both starch and MMT-Na, this nanofiller was expected to give an enhanced nano-dispersion state. These materials were prepared with solvent [121,122,131,132,142,144,145] or melt blending process [49–51,123–127,129,130,140,147]. It was highlighted that for glycerol content higher than 10 wt%, such systems led to the formation of an intercalated structure with d_{001} increased from 1.2 to 1.8 nm. This d_{001} value is already well reported into the literature and generally attributed to glycerol intercalation [50,131,142]. Similar morphology was obtained with sorbitol as the plasticizer [133] However, for glycerol content lower than 10 wt%, Tang et al. [142] have obtained an intercalated/exfoliated structure, meaning that the clay exfoliation process is likely perturbed by the polyol plasticizer content. On this way, Dean et al. have elaborated amylocorn starch nano-biocomposites by solvent [134] and melt [146] processes, with water as the sole plasticizer, to obtain a homogeneous dispersion with an intercalated or exfoliated structure. In addition, Chaudhary [143] has obtained an intercalated/exfoliated morphology with the melt dispersion of a hydrophobic nanofiller, OMMT-Alk4, without polyol plasticizer. These results confirm the strong influence of the polyol plasticizer on the exfoliation process and thus on the resulting morphology. This behavior is likely related to the hydrogen bonds established between glycerol and MMT platelets, which could disturb the clay exfoliation process [121,130,131].

To overcome these limitations induced by polyol plasticizers, some authors replaced these plasticizers by urea [128,142], urea/ethanolamine [135], formamide [142], formamide/ethanolamine [138,139] or urea/formamide [136,137]. MMT-Na dispersion into these urea or formamide plasticized starch matrices by solvent [142] or melt [128] process led to the formation of intercalated structures. Thus, to increase the clay/matrix affinity, different organo-modified MMT have been incorporated namely, OMMT-EtA [135,138,139], OMMT-CitA [136,137] and OMMT-Bz2 [128]. These OMMT were incorporated into the urea, urea/ethanolamine, formamide/ethanolamine or urea/formamide plasticized starch by melt process. The incorporation of OMMT-EtA into formamide/ethanolamine or urea/ethanolamine plasticized matrices led to intercalated structures with d_{001} = 2.6 nm [138,139] and exfoliation [135], respectively. In the same way, exfoliated nano-biocomposites have been obtained with the dispersion of OMMT-CitA [136,137] and OMMT-Bz2 [128] into urea/formamide and urea plasticized starch, respectively. Such an exfoliated structure has been obtained even for clay content higher than 5 wt%. Thus, it has been demonstrated that with the modification of the plasticizer and clay polarity, exfoliation can be reached. Nevertheless, these compounds are eco-toxic and cannot be used to elaborate safe biodegradable "green" materials.

On this way, Kampeerappun et al. [122] have focused their attention on the use of a new eco-friendly compatibilizer, chitosan, to promote the MMT platelets exfoliation. Thus, they have prepared cassava starch/chitosan/MMT-Na nano-biocomposites by casting. The nano-biocomposites were prepared with the

mixing of starch with chitosan powder (varied from 0 to 15 wt% of starch) and MMT-Na (varied from 0 to 15 wt% of starch). Only a small increase in the clay d_{001} from 1.2 to 1.4–1.5 nm was achieved since the molecular mass of the chitosan used was too high to be easily intercalated into the MMT inter-layer spacing. However, these authors assumed that this polycation can act as a compatibilizing agent leading to few clay aggregates and improved mechanical properties.

This strategy, namely the use of cationic polysaccharide surfactant to promote the clay exfoliation process, was successfully applied by Chivrac et al. [147] with cationic starch (CS) as MMT organo-modifier. After organo-modification, this nanofiller was incorporated into glycerol plasticized wheat starch by mechanical kneading into an internal batch mixer at low temperature (70 °C) to produce nano-biocomposite materials. According to Chivrac et al. [147], no diffraction peak was observed by X-ray diffraction, suggesting an exfoliated morphology (Fig. 7). Moreover, TEM analyses confirmed the nanoscaled dispersion and showed that the use of this surfactant led to a non-aggregated structure. These authors assumed that this dispersion state is achieved thanks to the preferential interactions established between the hydroxyl groups of the different starches-based biomacromolecules.

The different morphologies obtained with all these plasticized starch matrices and various nanofillers are summarized in Tables 5 and 6.

Park et al. [49,50] have shown with DMTA analyses that potato starch/OMMT-OH1 nano-biocomposites displayed higher elastic modulus compared to those elaborated with OMMT-Bz or OMMT-Alk2. This behavior was explained by the poor nanofiller dispersion and the lack of compatibility between the plasticized starch and these more hydrophobic organo-clays. Surprisingly, these hybrid materials displayed lower elastic modulus compared to the virgin matrix. Such a result was unexpected since the nanoplatelets generally induce a stiffness increase. This behavior was explained by a shift of the relaxation peaks toward lower temperatures, observed on tan δ, suggesting a matrix plasticization. This assumption is consistent with the nanofiller excess of surfactants, which may diffuse into the matrix and plasticize it. The highest elastic moduli were obtained with MMT-Na. This behavior is linked to the reinforcing effect of the clay and to a shift of the tan δ peaks toward higher temperatures, which indicates that clay layers strongly influence the starch chain mobility. This tendency was attributed to the MMT-Na higher affinity with the starch chains. The same trends were observed by DSC [137], meaning that starch/clay hybrids were strongly affected by the clay surface polarity and the clay/matrix interactions. Besides, Chiou et al. [123] analyzed the thermo-mechanical properties of wheat starch/MMT-Na nano-
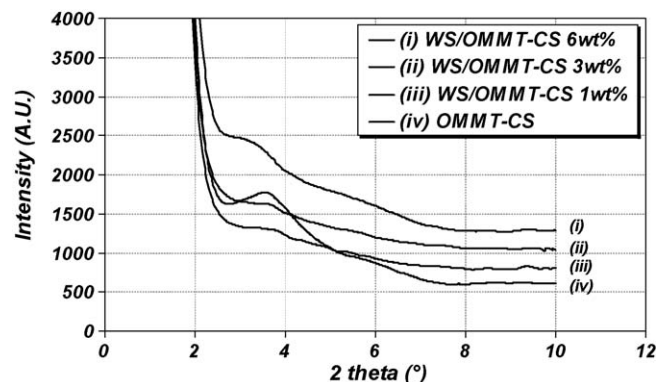

Fig. 7. XRD patterns for OMMT-CS and WS/OMMT-CS nano-biocomposites with 1, 3 and 6 wt% of clay inorganic fraction [147].

Table 5
Morphology of the plasticized starch nano-biocomposites elaborated by solvent process.

Plasticizer	Nanofillers	Morphology	References
Only water	MMT-Na	Intercalated	[134]
		Exfoliated	[134]
Glycerol content < 10 wt%	MMT-Na	Intercalated/Exfoliated	[142]
Glycerol content > 10 wt%	OMMT-Alk5	Intercalated	[141]
	MMT-Na	Intercalated, $d_{001} \sim 1.8$ nm	[121,122,131,132,142,144,145]
	MMT-Na/Chitosan	Intercalated, $d_{001} \sim 1.5$ nm	[122]
Urea	MMT-Na	Intercalated, $d_{001} \sim 2.3$ nm	[142]
Formamide	MMT-Na	Intercalated, $d_{001} \sim 2.3$ nm	[142]

biocomposites and observed that elastic modulus did not depend on the high frequency solicitations. This behavior indicates that these samples formed a gel-like structure and had a better dispersion state than the more hydrophobic nanofillers [123,162].

The Young's modulus of wheat and corn starch-based nano-biocomposites elaborated with MMT-Na and OMMT-CS has been studied by uniaxial tensile tests. These materials displayed substantial improvement in mechanical properties correlated to the clay loading for MMT-Na [125,144,147] (with corn and wheat starch). These stiffness increases were linked to the nanofiller rigidity and dispersion state and to the specific interactions established between the nanofiller surface and the matrix [163]. These increases were more pronounced for the well exfoliated nanofiller OMMT-CS than for the MMT-Na.

Park et al. [49] have determined the mechanical behavior of potato starch nano-biocomposites elaborated with OMMT-Alk2, OMMT-Bz, OMMT-OH1 and MMT-Na. It was clearly seen that the most hydrophobic nanofillers (OMMT-Alk2, OMMT-Bz) displayed lower tensile strength and strain at break compared to the neat matrix. This behavior was induced by the huge clay aggregates, which generate internal stress at the clay/matrix interface and thus enhanced the material embrittlement. For OMMT-OH1, higher tensile strength properties were obtained thanks to its higher dispersion state. The MMT-Na hybrids showed the highest tensile strength and strain at break, higher than the neat matrix ones. These results were partially contradicted by those of Chivrac et al. [147], Lilichenko et al. [144] and Mondragon et al. [145]. These different authors have reported a decrease in the strain at break of starch/MMT-Na nano-biocomposites. These differences were not explained but could be linked to the differences in the starch botanical origin and/or to the plasticizer content. Besides, Chivrac

et al. [147] have demonstrated that the incorporation of OMMT-CS did not alter the strain at break of the plasticized starch-based nano-biocomposites. Consequently, these studies highlight the possibility, for well exfoliated nanofillers, to harden the plasticized starch materials without affecting their strain at break.

Some authors studied in details the thermal stability of starch-based nano-biocomposites. Park et al. [50] showed by TGA that the potato starch/MMT-Na and OMMT-OH1 hybrids had a higher degradation temperature in comparison to the neat matrix. This increase in the thermal stability was significant up to 5 wt% of clay for either MMT-Na or OMMT-OH1, while this increase was leveled off with further increases in clay content. Moreover, the potato starch/MMT-Na thermal stability was higher than the OMMT-OH1 nano-biocomposites one. Such results highlighted some relation-ships between the MMT dispersion and the thermal stability. The same tendency was observed with other studies based on various starches and nanofillers [50,132,133]. These results assessed for an enhancement of the material thermal stability induced by the MMT. This behavior is commonly observed in nanocomposite systems and is linked to the clay aspect ratio and dispersion state. The exfoliation of the MMT nano-platelets into the matrix increases the tortuosity of the combustion gas diffusion pathway and favors the formation of a char at the material surface [19].

The nanofiller is also known to greatly influence the water vapor permeability of the nano-biocomposite materials. Park et al. [49] examined the potato starch nano-biocomposite water vapor permeability with different clays. According to the presented results, all the hybrid films showed lower water vapor perme-ability compared to the pristine matrix. For instance, the MMT-Na hybrid water vapor permeability has been reduced by nearly a half compared to the pristine matrix with 5 wt% of clay loading. The

Table 6
Morphology of the plasticized starch nano-biocomposites elaborated by melt process.

Plasticizer	Nanofillers	Morphology	References
Only water	MMT-Na	Exfoliated	[146]
	OMMT-Alk4	Intercalated–Exfoliated	[143]
Glycerol content > 10 wt%	OMMT-Bz	Microcomposite	[49,123]
	OMMT-Alk1	Microcomposite	[123]
	OMMT-Alk2	Microcomposite	[49]
	OMMT-Alk7	Intercalated, $d_{001} \sim 3.4$ nm	[125]
	OMMT-OH1	Intercalated, $d_{001} \sim 2.0$ nm	[49,50,123,126]
	MMT-Na	Intercalated, $d_{001} \sim 1.8$ nm	[49–51,123–127,129,130,140,147]
	OMMT-CS	Exfoliated	[147]
Sorbitol	MMT-Na	Intercalated, $d_{001} \sim 1.8$ nm	[133]
Urea	MMT-Na	Intercalated, $d_{001} \sim 1.8$ nm	[128]
	OMMT-Bz2	Exfoliated	[128]
Urea/Ethanolamine	OMMT-EtA	Exfoliated	[135]
Formamide/Ethanolamine	OMMT-EtA	Intercalated, $d_{001} \sim 2.6$ nm	[138,139]
Urea/Formamide	OMMT-CitA	Exfoliated	[136,137]

same trends are observed into other plasticized starch nano-biocomposites [50,135]. This behavior is induced by two distinct phenomena, namely (i) the dispersion of the silicate layers and (ii) the solubility of the penetrant gas into the nano-biocomposite films [19]. Thus, for the micro-biocomposites based on OMMT-Bz, OMMT-Alk2 or OMMT-OH1 the barrier properties enhancements were linked to decreases in the water solubility due to the surfactant hydrophobic character. On the contrary, for MMT-Na, the permeability decrease likely resulted from the better nano-dispersion. Finally, Cyras et al. [132] and Mondragon et al. [145] have highlighted the clay influence on the water content, at equilibrium. According to these authors, the higher is the clay content, the lower the water content is. This behavior was likely induced by the nanofiller, which modified the water solubility thanks to its dispersion state.

To conclude, these different studies have clearly demonstrated the possibility to exfoliate MMT nanofillers into plasticized starch matrices with solvent and melt processes. The resulting properties (mechanical, barrier, thermal stability, etc.) of the corresponding nano-biocomposites are largely enhanced and point out the great potential of these innovative materials. However, the negative impact of the starch plasticizers on the clay intercalation/exfoliation process has also been clearly highlighted. Thus, to fully describe and understand the starch nano-biocomposite materials, future studies should be focused on the analyses of the clay/plasticizer/matrix interactions, species mobility and local nanostructures with advanced characterization techniques.

3.1.3.2. Starch blends-based nano-biocomposites. An usual answer to the water sensitivity and poor mechanical properties of the starch-based materials is the development of multiphase materials such as starch/polymer blends [164]. Tapioca starch/PLA nano-biocomposites (90/10 wt%/wt%) have been elaborated by Lee et al. [148–151] by melt process. The dispersion of hydrophobic nanofillers, namely, OMMT-Bz, OMMT-Alk1, OMMT-Alk3, OMMT-Alk4 and OMMT-Alk7 led to intercalated nano-biocomposites with $2.9 < d_{001} < 3.4$ nm. Intercalated morphologies have also been obtained with the more hydrophilic OMMT-OH1. These intercalated morphologies are related to the high starch content of these blends, which is known to hinder the clay exfoliation process of the hydrophobic clays [49,50].

After MMT-Na incorporation, nano-biocomposites displayed an intercalated structure with $d_{001} \sim 2.3$ nm. Similar results were obtained with amylocorn starch/PVAL nano-biocomposites elaborated by melt process [146]. High intensity and sharp diffraction peak ($d_{001} \sim 1.8$ nm) was obtained with the inclusion of PVAL leading to a highly ordered-intercalated and non-exfoliated structure, as pointed out by TEM analyses (Fig. 8). Since Dean et al. [134,146] have reported the formation of well exfoliated structure for amylocorn starch/MMT-Na nano-biocomposites elaborated without non-volatile plasticizer, these results may indicate a restriction of the MMT-Na intercalation/exfoliation process induced by PLA and PVAL. For PLA, the lack of compatibility with MMT-Na explains this trend [165]. For PVAL, infrared spectroscopy analyses have evidenced hydrogen bonds between MMT-Na and PVAL chains, which likely maintain the tactoïds organization [146].

Starch/PCL nano-biocomposites have also been elaborated by melt blending process. McGlashan and Halley [157] demonstrated that, depending on the PCL/starch ratio, the OMMT-OH1 incorporation led to intercalated or exfoliated nano-biocomposites [157]. For PCL content higher than 70 wt%, a clay exfoliated state was obtained. Then, with a starch content increase, a diffraction peak corresponding to an intercalated structure appeared with a $d_{001} \sim 4.0$ nm and with an intensity correlated to the starch content. Since OMMT-OH1 is easily exfoliated into PCL and mainly
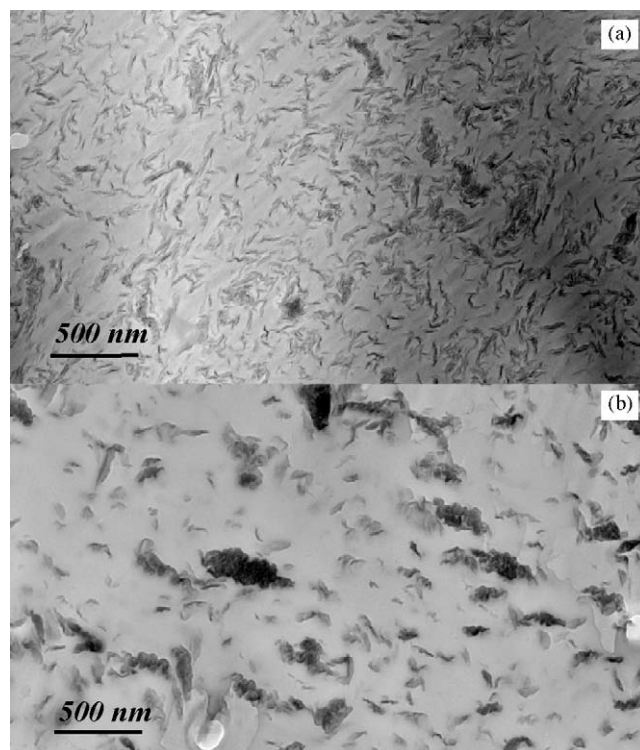

Fig. 8. TEM micrographs of (a) amylocorn starch nanocomposite with 2.5 wt% of MMT-Na content and (b) amylocorn starch/PVAL nanocomposite with 5 wt% of PVAL and 2.5 wt% of MMT-Na content [146].

intercalated into plasticized starch, one may suppose that these nanofillers were mainly dispersed into the PCL domains. These results have been confirmed by Perez et al. [152,154,155], who reached exfoliation for high PCL content with OMMT-OH1. The same dispersion state has been achieved with OMMT-Bz has the nanofiller for high PCL content. According to Perez et al. [152,154–156], such morphology is favored by the good nanofiller/PCL affinity, which promotes the clay exfoliation. Besides, Kalambur and Rizvi [158,159] obtained microcomposites with the dispersion of OMMT-Alk5 into starch/PCL blends plasticized with glycerol. This morphology was related to the low matrix/nanofiller affinity and to the glycerol which is known to restrict the clay platelets delamination [142].

Finally, the MMT-Na dispersion led to an intercalated structure with a $d_{001} = 1.8$ nm. According to Perez et al. [152–155], since the diffraction peak intensity was low, the existence of intercalated/exfoliated structure is possible but not fully proved.

The different morphologies obtained in these blends are summarized in Table 7.

The uniaxial tensile properties of starch/PCL nano-biocomposites have been measured and have shown that, whatever the clay type, the incorporation of the nanoclays led to an increase in the material rigidity, related to the clay modulus and clay/matrix interactions [152,157]. Perez et al. [152,154] have demonstrated that the most significant stiffness enhancements were obtained with OMMT-Bz. This result was attributed to the high compatibility OMMT-Bz/PCL, which led to an exfoliated morphology. In the same way, McGlashan and Halley [157] reported significant stiffness improvement with OMMT-OH1 correlated to the clay dispersion state. The highest mechanical reinforcing efficiencies were observed for the exfoliated blends obtained with high PCL content. Then, the starch content increase led to a lower stiffness increase. Starch blends elaborated with PLA [149,151] or PVAL [146] also shown an increase in the Young's modulus related to the

Table 7
Morphology of the starch-blends nano-biocomposites elaborated by melt process.

Polymer into the starch blend	Nanofillers	Morphology	References
PLA content = 10 wt%	MMT-Na	Intercalated, $d_{001} \sim 2.3$ nm	[148,149]
	OMMT-OH1	Intercalated	[148,150]
	OMMT-Bz	Intercalated, $d_{001} \sim 3.4$ nm	[151]
	OMMT-Alk1	Intercalated, $d_{001} \sim 3.2$ nm	[151]
	OMMT-Alk3	Intercalated	[148]
	OMMT-Alk4	Intercalated, $d_{001} \sim 2.9$ nm	[151]
	OMMT-Alk7	Intercalated, $d_{001} \sim 3.2$ nm	[151]
PVAL content < 7 wt%	MMT-Na	Intercalated, $d_{001} \sim 1.8$ nm	[146]
PCL content > 70 wt%	MMT-Na	Intercalated, $d_{001} \sim 1.8$ nm	[152–155]
	OMMT-Bz	Exfoliated	[152,154–156]
	OMMT-OH1	Exfoliated	[152,154,155,157]
PCL content < 70 wt%	OMMT-OH1	Intercalated, $d_{001} \sim 4.0$ nm	[157]
PCL and Glycerol	OMMT-Alk5	Microcomposite	[158,159]

clay content. As usual, these increases are linked to the clay stiffness and dispersion state.

The nanoclay effect on the strain at break properties is also very significant. For PCL [154,157] or PVAL [146] blends, a huge increase due to the clay introduction into the matrix was reported. Dean et al. showed that, the strains at break of starch nano-biocomposites filled with 2 wt% of PVAL were generally lower than those without. However, with 5 wt% of PVAL, the strain at break increased (Table 8). These trends were linked to the clay/PVAL interactions. At 2 wt%, the PVAL chains were tightly bound to the MMT-Na generating aggregations. At higher PVAL content, 'free' PVAL chains result in material plasticization.

The effects of these nanofillers on the blends thermal properties were studied by DSC. Perez et al. [153,155] have shown a significant effect of MMT-Na, OMMT-OH1 and OMMT-Bz on the PCL crystallization process, these nanofillers acting like nucleating agents. As the blend was cooled from the molten state, the platelets generated nucleation sites leading to a crystallization temperature increase. However, restrictions in chain mobility due to the presence of exfoliated platelets reduced the degree of crystallinity and altered the crystallization mechanism. The same trends were also reported by McGlashan and Halley [157] and Kalambur and Rizvi [159] with, respectively, OMMT-OH1 and OMMT-Alk5. Finally, for starch/PCL blends, Perez et al. [154] have clearly highlighted a decrease in the water uptake and water diffusion coefficient linked to the clay content and dispersion state.

To conclude, well exfoliated starch/PCL nano-biocomposites displaying enhanced properties have been elaborated with high PCL content. However, with the increase in the starch content, the nano-hybrid materials become more and more intercalated. This trend is likely related to the nanofiller polarity, which led to a poor starch/MMT affinity. The dispersion of a mix of hydrophilic and hydrophobic nanofillers, which can respectively be exfoliated both into the carbohydrate phase and into a more hydrophobic biopolymer matrix, could be a powerful answer to obtain a more homogeneous MMT nano-dispersion even at high starch content.

3.1.3.3. Modified starch-based nano-biocomposites. To decrease the starch-based material water sensitivity, another approach consists in the chemical modification of the starch chains. The objective of this chemical modification is the substitution of hydroxyl groups by less hydrophilic functions, such as acetate groups [166]. Qiao et al. [160] have elaborated, into an internal batch mixer, acetylated starch nano-biocomposites with 5 wt% of MMT-Na and OMMT-Alk6 using glycerol as plasticizer. Besides, Xu et al. [161] have elaborated, by melt extrusion, acetylated starch nano-biocomposite foams with 5 wt% of OMMT-OH1, OMMT-Bz, OMMT-Alk3 or OMMT-Alk4.

The morphological analyses carried out on these nano-biocomposites have demonstrated that the MMT-Na incorporation into this more hydrophobic matrix (compared to unmodified starch) led to an intercalated structure displaying an intense and sharp diffraction peak. This peak, corresponding to a d_{001} of 1.8 nm, was assigned to glycerol intercalation [126,167]. The morphological analyses carried out on samples prepared with the rather hydrophobic nanofillers have highlighted that the intercalation extent follows the sequence, OMMT-OH1 > OMMT-Bz ~ OMMT-Alk3 > OMMT-Alk4 > OMMT-Alk6 (Table 9) [160,161].

The effect of MMT on uniaxial tensile properties of acetylated starch nano-biocomposites was investigated by Qiao et al. [160]. They reported an increase in the tensile strength with the addition of 5 wt% of MMT-Na or OMMT-Alk6. On the contrary, the strain at break properties of these nano-biocomposites were depressed, the lower strain at break values being obtained with OMMT-Alk6. This trend was linked to the corresponding highly intercalated structure.

The nanofiller influence on the thermal behavior was analyzed by Qiao et al. [160] using DMTA. The different samples exhibited a relaxation transition at 50 °C, corresponding to the glassy state transition of the starch-rich phase. The relaxation of acetylated starch/clay nano-biocomposites shifted towards higher temperature, compared to the neat matrix. Thus, it has been concluded that the presence of clay reduced the chain mobility and increased the

Table 8
Uniaxial tensile parameters of starch/PVAL blends filled with MMT-Na [146].

Samples composition in weight (starch/PVAL/MMT-Na)	Young's modulus (MPa)	Strain at break (%)
100/0/0	3085	8.7
100/0/2.5	4212	6.0
100/0/5	4612	4.2
100/2/0	2808	8.3
100/2/2.5	4947	5.8
100/2/5	5429	4.2
100/5/0	2955	10.0
100/5/2.5	5429	9.4
100/5/5	5250	8.6
100/7/0	3176	10.3
100/7/2.5	4008	9.2
100/7/5	4677	8.7

Table 9
Morphology of the acetylated starch nano-biocomposites elaborated by melt process.

Nanofiller	Morphology	References
MMT-Na	Intercalated, $d_{001} \sim 1.8$ nm	[160]
OMMT-Alk6	Intercalated, $d_{001} \sim 3.1$ nm	[160]
OMMT-Alk4	Intercalated, $d_{001} \sim 3.5$ nm	[161]
OMMT-Alk3	Intercalated, $d_{001} \sim 3.8$ nm	[161]
OMMT-Bz	Intercalated, $d_{001} \sim 3.8$ nm	[161]
OMMT-OH1	Intercalated, $d_{001} \sim 4.0$ nm	[161]

T_g of the starch-rich phase. Moreover, these authors assumed that the temperature shift of the acetylated starch/OMMT-Alk6 samples was still higher than with MMT-Na because of the easier intercalation into OMMT-Alk6 layers.

Such behavior was confirmed by Xu et al. [161] who analyzed the T_g of the acetylated starch nano-biocomposites by DSC. According to these authors, the T_g of starch acetate was increased by the addition of organo-clay. The greatest increase was recorded with the incorporation of OMMT-OH1, whereas the smallest increase was observed for OMMT-Alk4. The authors attributed this T_g increase to the formation of an intercalated structure, which restricted the movement of starch acetate chains. Moreover, the different increases in T_g observed with the addition of various organo-clays were explained by the different levels of compatibility between starch acetate and organo-clays.

The study of the nanofiller influence on the starch acetate nano-biocomposites thermal stability has shown an enhancement of this property linked to the increase in the tortuosity of the combustion gas diffusion pathway [161]. However, the best thermal stability was not achieved with the most homogeneously nano-dispersed clay, namely OMMT-OH1, but with OMMT-Alk4. According to the authors, a possible reason for this difference was the higher thermal stability of the organic modifiers in OMMT-Alk4 compared to OMMT-OH1.

To conclude, these studies have highlighted that, in acetylated starch, the best clay nano-dispersion is achieved with OMMT-OH1. This result is linked to the rather hydrophobic behavior of this matrix in comparison to unmodified starch, which leads to a lack of compatibility with more hydrophilic nanofillers, such as MMT-Na. Nevertheless, even if a good nano-dispersion is obtained with OMMT-OH1, the corresponding nano-biocomposites only displayed an intercalated structure. Consequently, to obtain an exfoliated state, new organo-modified nanofillers should be considered. In addition, until now, studies have only been focused on the use of acetylated matrices. Other modified starch matrices could also be used, such as methylated or carboxymethylated starch.

3.2. Cellulose

Cellulose is the most abundant biopolymer in the biosphere. Often associated with lignins (ligno-cellulose products), this carbohydrate polymer is the main constituent of wood, flax, ramie, hemp or cotton (Table 10).

3.2.1. Cellulose structure

This biopolymer is a linear macromolecule constituted of D-glucose units (cellobiose) linked by $\beta(1 \rightarrow 4)$ linkages and shows a semi-crystalline structure. The glucose monomers units in cellulose form both intra- and inter-molecular hydrogen bonds generating cellulose microfibrils. These hydrogen bonds lead to the formation of a linear crystalline structure with a high theoretical tensile strength [168]. Four principal allomorph structures have been identified for cellulose [169–172]:

 (i) Cellulose I crystal structure, which is the natural form of the cellulose, is the result of the co-existence of two distinct crystalline forms named cellulose I_{α} and I_{β}, which have respectively a triclinic and a monoclinic unit cell.
 (ii) Cellulose II is generally obtained by regeneration of cellulose I from solution. This allomorph is known by the term "regenerated" cellulose. The transition from cellulose I to II is not reversible.
(iii) Cellulose III is prepared from celluloses I and II with liquid ammonia or ethylene diamine treatment. These two celluloses are named cellulose III_I and III_{II}, respectively.
(iv) Cellulose IV is prepared with glycerol at high temperature from Cellulose III. Here again two types exist: cellulose IV_I and IV_{II} obtained from cellulose III_I and III_{II}, respectively.

Depending on their origin, cellulose microfibrils have diameters in the range 2–20 nm while their length can attain several tens of microns [173]. The microfibrils cellulose chains are aligned in parallel in an almost perfect crystalline array. Some imperfections arise from dislocations at the interface of microcrystalline domains along the microfibril length [174]. These imperfections are advantageously used to produce, by acid treatment, rod-like mono-crystals called whiskers having the same diameter as the starting microfibrils but shorter length. These cellulose whiskers show a mechanical modulus of about 130 GPa [175]. Thanks to these characteristics (microscopic dimensions, form and exceptional mechanical properties), these whiskers can be incorporated as a reinforcing component into polymer matrices to produce nanocomposite materials with enhanced properties for a wide range of potential applications [176].

The numerous hydroxyl functions in cellulose result in strong hydrogen bonds, creating a physical network, which makes the material non-fusible [177]. To produce plastic materials from cellulose, a chemical modification has to be performed. This modification often consists in the replacement of the cellulose hydroxyl functions, by acetate or methyl functions. The objective of this modification is the decrease in the hydrogen bonds intensity.

3.2.2. Modified cellulose-based nano-biocomposites

Only few cellulose acetate (CA) nano-biocomposites have been elaborated, studied and reported in the literature [178–182]. Park et al. [178] and Wibowo et al. [179] have elaborated CA/OMMT-OH1 nano-biocomposites, by melt blending process, with various contents of triethyl citrate (TEC) as plasticizer. Different morpho-

Table 10
Composition of ligno-cellulosic fibers, from various botanical sources [212].

Fibers	Cellulose content (%)	Lignin content (%)	Hemicellulose content (%)	Ash (silica, etc.) (%)
Straw fibers:				
Wheat	29–35	16–21	27	5–9
Rice	28–36	12–16	23–28	15–20
Rye	33–35	16–19	27–30	2–5
Wood fibers:				
Conifers	40–45	36–34	7–14	<1
Leafwood	38–49	23–30	19–26	<1
Others:				
Flax	43–47	21–23	16	5
Jute	45–53	21–26	15	0.5–2
Cotton linters	90–85	/	1–3	0.8–2

Table 11
Morphology of the CA/OMMT-OH1 nano-biocomposites.

CA nano-biocomposites with:	Elaboration process	Morphology	References
TEC content < 20 wt%	Melt process	Exfoliated	[178,179]
TEC content > 20 wt%	Melt process	Intercalated, $d_{001} \sim 4.0$ nm	[178,179]
TEC Plasticized = 25 wt% and CAB-g-MA 5 wt%	Melt process	Exfoliated	[180,181]
PCL content = 80 wt%	In situ polymerization and solvent process	Exfoliated	[182]

logical analyses, such as XRD experiments, have been performed. According to the results, nano-biocomposites with 20 wt% of TEC plasticizer and 5 wt% of OMMT-OH1 displayed an exfoliated structure. In comparison, nano-biocomposites having 30–40 wt% of plasticizer displayed an intercalated structure with a d_{001} = 4.0 nm. Moreover, the higher the TEC content, the higher the diffraction peak intensity. This behavior is related to the hydrogen bonds established between the –OH groups of the TEC plasticizer and those of the organo-modifier in OMMT-OH1, which disturb the intercalation/exfoliation process. Thus, OMMT-OH1 seems suitable to achieve exfoliation in CA nano-biocomposites but only at low TEC content.

To enhance the clay exfoliation process, even for high plasticizer content, Park et al. [180,181] have elaborated CA-based nano-biocomposites with a carbohydrate compatibilizer, cellulose acetate butyrate grafted maleic anhydride (CAB-g-MA). This compatibilizer was synthesized by radical graft polymerization of maleic anhydride (MA) monomers onto cellulose acetate butyrate (CAB). This grafting was conducted by melt process compounding with (2,5-dimethyl-2,5-di(tert-butylperoxy)hexane). The same blends as those previously presented [178,179] were elaborated with a CA/TEC ratio of 75/25 wt%/wt%. The mixtures were mixed with 5 wt% of OMMT-OH1 and between 0 and 7.5 wt% of CAB-g-MA and then melt compounded. Without CAB-g-MA, the nano-biocomposites displayed an intercalated structure with a d_{001} = 4.0 nm. On the contrary, an exfoliated state was achieved with this compatibilizer, the best exfoliated state being obtained with 5 wt% of CAB-g-MA.

To achieve exfoliation into CA-based nano-biocomposites, Yoshioka et al. [182] developed a different approach. These authors used a hybrid elaboration protocol between the in situ polymerization and the solvent intercalation process. Their objective was to obtain grafted poly(ε-caprolactone) (PCL) chains to facilitate the clay delamination process. According to the presented results, a well exfoliated nano-biocomposite is obtained for OMMT-OH1. Nevertheless, these materials are composed of 80 wt% of PCL and then, the CA content is rather low.

The different morphologies obtained with these CA-based nano-hybrid materials are summarized in Table 11.

The effect of clay dispersion state on the main properties of CA-based nano-biocomposites has been studied with various techniques. Park et al. [178] observed a sharp increase in the notched izod impact strength and the tensile strain at break of the CA/OMMT-OH1 hybrid materials correlated to the increase in plasticizer content. As expected, the clay nanoplatelets incorporation increased the tensile modulus of the CA hybrids (compared to pristine matrix, Fig. 9). Park et al. also studied the tensile and flexural properties of the plasticized CA/OMMT-OH1 hybrids with various MA-g-CAB contents [180,181]. According to the presented results, the best mechanical properties enhancements are obtained with the exfoliated morphology, with 5 wt% of MA-g-CAB. At higher compatibilizer content, the mechanical properties decreased. Since it has been clearly demonstrated in different nanocomposite systems that, the better the dispersion, the better the resulting mechanical properties improvement [19–21], these mechanical properties variations are linked to the MMT dispersion state.

The nanofiller dispersion effect on T_g has also been studied by DMTA. Park et al. [178] have shown that the higher the plasticizer content, the lower the T_g (130 and 86 °C for CA/TEC ratio of 80/20 and 60/40 wt%/wt%, respectively). An increase in the nano-biocomposite T_g was observed after incorporation of the nano-platelets [178,180]. This trend is likely related to the clay dispersion state, which can hinder the polymer chains mobility. Another possible explanation is linked to the hydrogen bonds, which could be established between the –OH groups of the organo-modifier and those of the carbohydrate chains and which could reduce the CA mobility.

Besides, water vapor permeability was examined in a controlled temperature and relative humidity chamber [178]. A strong decrease in permeability, reaching 2-fold at the highest organo-clay content, was observed. This decrease was due to the well-ordered and dispersed silicate layers having a large aspect ratio, which lead to a more tortuous path for the diffusion of gas molecules through the film [183].

To conclude, these studies have shown that exfoliation can be reached in CA nano-biocomposite materials. Nevertheless, a negative effect of the plasticizer on the MMT exfoliation process has been highlighted. This limitation has been overcome thanks to the use of a carbohydrate compatibilizer, which modifies the clay/matrix interface. However, only OMMT-OH1 has been tested into CA matrices. To reach a full exfoliation, new OMMTs prepared with carbohydrate surfactants should also be tested. Exfoliation has been also obtained with CA/PCL blends. However, the morphology is mainly achieved thanks to the high PCL content.

3.3. Chitin and chitosan

Chitin is the second most abundant agro-polymer produced in the nature after cellulose. It appears in nature as ordered crystalline microfibrils forming structural components in the exoskeleton of arthropods or in the cell walls of fungi and yeast [184,185]. It is an acetylated polysugar composed of N-acetyl-D-glucosamine groups linked by $\beta(1 \rightarrow 4)$ linkages (Fig. 10). From chitin, chitosan is obtained by deacetylation.

3.3.1. Chitin and chitosan structures

Depending on the source, chitin occurs as two allomorphs forms named α and β [186]. A third allomorph structure chitin γ has also been reported, but is seems that it is a variant of the α form [187].
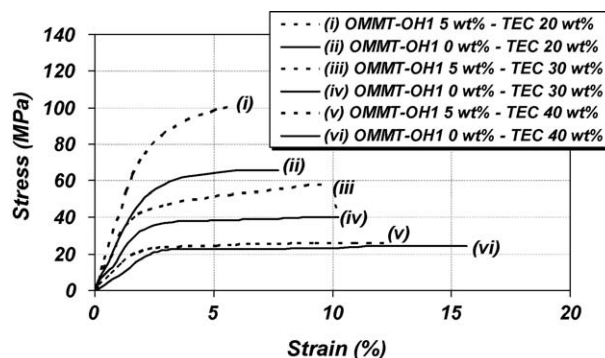

Fig. 9. Cellulose acetate nano-biocomposite tensile curves for different plasticizer (TEC) and clay contents.
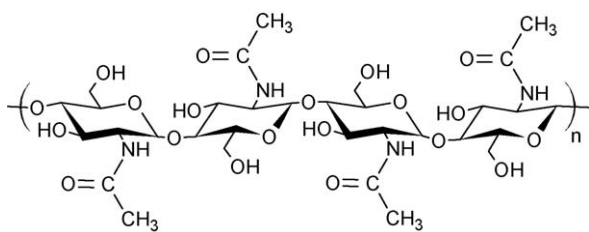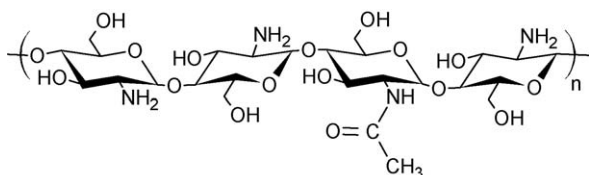
Fig. 10. Chitin chemical structure.

Fig. 11. Chitosan chemical structure.

These two structures are organized in crystalline sheets where numbers of intra-sheet hydrogen bonds tightly hold them. The α form presents some inter-sheets hydrogen bonds. Such a feature is not found for the β form, which is consequently more prone than the α form to water swelling [188,189]. Like cellulose, the semi-crystalline structure of chitin microfibrils can be treated with acid to produce whisker-shaped nanofillers that can be incorporated into polymers to elaborate nano-hybrid materials [190,191].

Contrary to chitin, chitosan is not widespread in the nature. It is found in some mushrooms (zygote fungi) and into the termite queen's abdominal wall. It is industrially obtained by partial chitin deacetylation [192]. Its chemical structure, represented in Fig. 11, is a random linear chaining of N-acetyl-D-glucosamine units (acetylated unit) and D-glucosamine (deacetylated unit) linked by $\beta(1 \rightarrow 4)$ linkages.

Thanks to its amino group and compared to chitin, chitosan shows some particular properties. In acid conditions, when the amino groups are protonated, it becomes a water soluble polycation. Some polysaccharides can have a polyelectrolyte behavior, like carrageenan, but these agro-polymers are mainly polyanions [193]. The chitosan is characterized by its acetylation degree and by its molecular weight. These last parameters influence its viscosity and solubility. According to the bioresource, industrial chitosan shows molecular weights varying from 5000 to 1,000,000 g mol^{-1} and acetylation degrees from 2 to 60%.

In solid state, chitosan is a semi-crystalline polymer. Its morphology has been investigated and many allomorphs have been described, depending on its acetylation degree, on the distribution of the acetyl groups along the carbohydrate chain, on the chitosan preparation procedure [194,195].

3.3.2. Chitosan-based nano-biocomposites

Compared to the cellulose based-nano-biocomposites, a great number of chitosan-based nano-hybrids have been elaborated, studied and reported in the literature [122,196–203]. Chitosan/OMMT-OH1 nano-hybrid materials have been prepared into water by solvent process but led to the formation of highly flocculated systems. This morphology is obtained because OMMT-OH1 cannot be dispersed into water [197]. Besides, since chitosan is a polycation in acid conditions, it can be easily adsorbed on the MMT-Na surface. This property has been extensively used to elaborate chitosan/MMT-Na hybrid materials by solvent route. Solutions were prepared by chitosan addition into 1 or 2% (v/v) of acetic acid solution. MMT-Na was dispersed into water to obtain a 2 wt% clay suspension. To avoid any structural alteration of the phyllosilicate structure, the polysaccharide solution was adjusted with NaOH to pH 4.9 and

then was slowly added to the clay suspension at ambient temperature. This mixture was stirred and finally washed with purified water to remove acetate and then casted [196–199,201]. According to recent XRD experiments performed by Kampeera-pappun et al. [122], it has been claimed that chitosan did not diffuse into the clay inter-layers spacing. However, these results were contradicted by those of Darder et al. [196], which concluded to chitosan intercalation thanks to a shift of the MMT-Na diffraction peak to lower angles. Moreover, a broadening and intensity decrease in the diffraction peak was observed, indicating a disordered-intercalated/exfoliated structure [199,201]. Günister et al. [198] have studied the interactions between MMT-Na and chitosan by zeta potential measurements and have shown a chitosan ionic adsorption on the clay surface and an effective intercalation.

This inter-layer chitosan structure was studied by infrared spectroscopy [196,199], evidencing the adsorption of two chitosan layers on the clay surface and even inside the inter-layer spacing (Fig. 12). The first chitosan layer was mainly adsorbed thanks to electrostatic interactions between the chitosan –NH$_3^+$ groups and the MMT negative charges. The second layer adsorption was promoted by hydrogen bonds established between the chitosan amino and –OH groups and the clay substrate. At low MMT content, several authors have even shown the formation of an exfoliated nanostructure [197,201–203]. At higher MMT content, namely more than 5 wt%, the formation of intercalated/flocculated structure was observed [201].

Recently, Wang et al. [200] have introduced carboxymethyl groups into chitosan to enhance the hydrogen-bonding reaction between the matrix and –OH group located at the edges of MMT-Na. The corresponding nano-biocomposites were elaborated with a conventional solvent elaboration process, the MMT-Na being exfoliated into a large excess of water and then mixed with a solution of carboxymethylated chitosan. Nevertheless, this strategy has led to the formation of highly flocculated systems. According to the authors, this flocculated structure has been favored by the hydroxylated edge–edge interaction of the silicate layers. The different morphologies obtained in these systems are summarized in the Table 12.

The thermal transitions of these nano-biocomposites were investigated and related to the material dispersion state. Günister et al. [198] have measured the effect of the nanofiller addition on the T_g (by DSC) and observed an increase directly linked to the ionic interactions established between the chitosan and the nanofiller, which reduced the chains mobility.

As often depicted, increases in the tensile strength correlated to a small decrease in the strain at break were observed in the different chitosan nano-biocomposite [197]. These raises were induced by the nanofillers/chitosan interactions, which enhance the stress transfer at the interface. The strain at break decrease was related to the morphology of the chitosan/MMT hybrid materials which displayed, in the best case, an intercalated/exfoliated structure. Such a stiffness increase is already well reported into the literature and is correlated to the clay rigidity and dispersion state [204].

In addition, in vitro antimicrobial tests showed that chitosan/layered silicate nanocomposites had higher antimicrobial activity than pure chitosan. Thus, Wang et al. [202] and Lin et al. [203]

Table 12
Morphology of the chitosan nano-biocomposites elaborated by solvent process.

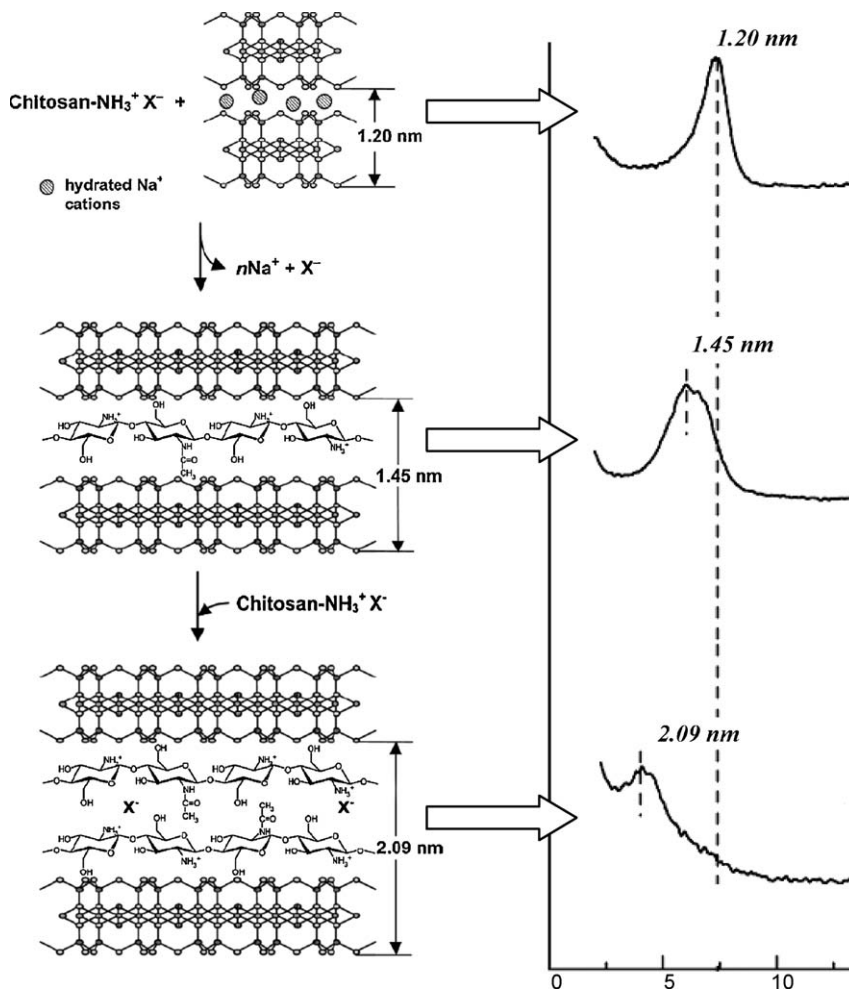| Matrices	Nanofillers	Morphology	References
Chitosan	OMMT-OH1	Microcomposite	[197]
	MMT-Na	Intercalated 1.4 nm $< d_{001} < 2.1$ nm	[196–201]
		Exfoliated	[197,201–203]
Carboxymethyl chitosan	MMT-Na	Microcomposite	[200]

Fig. 12. Intercalation of the chitosan layers into clay inter-layer spacing and the corresponding XRD patterns for MMT-Na (a) and chitosan nano-biocomposites prepared from chitosan/clay ratios of 0.5/1 (b) and 10/1 (c) [196].

concluded that these materials could be an interesting solution to develop new materials for biomedical applications as surgery.

To conclude, exfoliated chitosan nano-biocomposites displaying improved properties have been elaborated with MMT-Na. However, such nano-hybrids have only been prepared by solvent process. The elaboration of chitosan/polyester blends could be an interesting option to produce melt processable chitosan nano-biocomposites. Besides, to better understand the chitosan inter-calation process, nano-biocomposites should be prepared with various chitosan grades having different molecular weight, acetylation degree and distribution of the acetyl groups along the carbohydrate chain.

3.4. Pectin

Pectin is a linear macromolecule constituted of $\alpha(1 \rightarrow 4)$ linked D-galacturonic acid (Fig. 13). This monomer unit could be partially
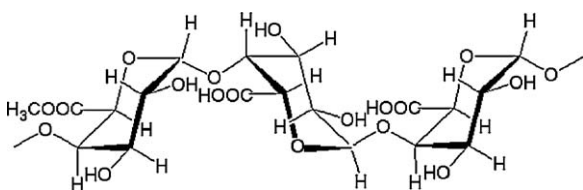

Fig. 13. Pectin chemical structure.

replaced by $\alpha(1 \rightarrow 2)$-linked L-rhamnose leading to a new structure named rhamnogalacturonan I. A third pectin structural type is rhamnogalacturonan II, which is a less frequent, complex and highly branched polysaccharide [205].

3.4.1. Pectin structure

In nature, around 80% of the galacturonic acid carboxyl groups are esterified with methanol. This proportion depends on the extraction conditions. Since, the ratio of esterified/non-esterified galacturonic acid determines the behavior of pectin in food applications, pectins are classified as high- or low-ester pectins [206]. The non-esterified galacturonic acid units can be either free acid or salts, with sodium, potassium or calcium as the counter ion. The partially esterified pectin salts are named pectinates. If the degree of esterification is below 5%, the salts are called pectates.

3.4.2. Pectin-based nano-biocomposites

Only few systems based on pectin nano-biocomposites have been elaborated, studied and reported in the literature with MMT-Na or OMMT-OH2 [207]. The elaboration protocol is a two steps procedure of ball milling followed by classical solvent elaboration process. First, the MMT and the pectin powders were mixed in the proper weight ratio in a stainless steel vial filled with tungsten carbide balls. The energy supplied during each impact of these tungsten carbide balls was used to decrease the polymer particles and the clay agglomerates size and to enhance the clay dispersion into the polymeric powder [208]. This pectin/clay powder was

Table 13
Morphology of pectin nano-biocomposites.

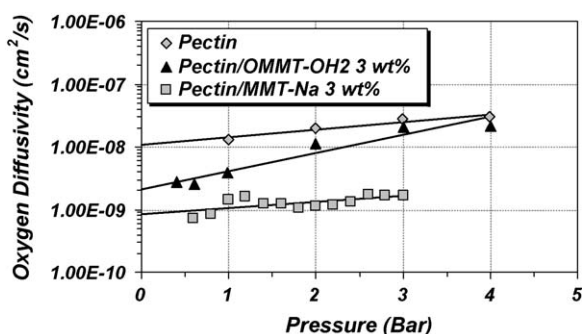| Elaboration technique	Nanofillers	Morphology	References
Ball milling and solvent process	MMT-Na	Exfoliated	[207]
	OMMT-OH2	Exfoliated	[207]

Fig. 14. Diffusion coefficients of oxygen in pectin samples at 25 °C from kinetic gravimetric sorption experiments.

milled. Then, sample films were prepared by dissolving milled pectin/clay in distilled water. The solutions were stirred and casted.

With OMMT-OH2, the results pointed out the major effect of the residence milling time on the resulting clay dispersion, a complete destructuration of the clay lamellar morphology being observed for high residence time. In similar condition, exfoliation state was also obtained with MMT-Na. The different dispersion states reached in these systems are summarized in the Table 13.

Contrary to pectin/OMMT-Na systems, tensile tests did not display a stiffness increase for pectin/OMMT-OH2 samples. According to Mangiacapra et al. [207], this behavior could be due to the higher affinity of the pectin with the MMT-Na platelets and a corresponding chain mobility decrease. Water and oxygen diffusion coefficients were determined for unfilled pectin and its nano-biocomposite materials. Decreases in these diffusion coefficients were pointed out for all the nano-biocomposites, whatever the nanoclay type. Moreover, the diffusion coefficients obtained for MMT-Na samples were lower than those of OMMT-OH2 ones (Fig. 14) [207]. Such results show that the unmodified clay had a better dispersion than OMMT-OH2, leading to an increase in the tortuosity of the diffusion pathway. No variation in the nano-hybrid degradation temperature measured by TGA was observed whatever the nanofiller and the experimental conditions (air or nitrogen).

To conclude, this study has demonstrated the interest in the ball milling process to obtain the MMT exfoliation with a pectin matrix. However, such elaboration is time and cost prohibitive. Consequently a melt approach should be developed to validate the potential of these nano-hybrid materials, e.g., with the elaboration of blends. In the same way, other nanofillers should be tested to understand better the effect of the nanofiller/matrix interface on the resulting properties.

4. Conclusions

This review aimed at presenting the actual state of the art of polysaccharides/nanoclay nano-biocomposites. These nano-hybrid materials mainly differ from conventional nanocomposites due to their hydrophilic character. Consequently, only micro-composite morphologies are reached with the dispersion of the common commercially available hydrophobic organo-modified nanoclays, such as Cloisite®-based MMT. On the opposite,

exfoliated structures are often obtained with more hydrophilic nanofillers, such as "natural" sodium MMT.

Because of the high thermal sensitivity of the carbohydrate chains, solvent intercalation process is often required or used for the nano-biocomposites elaboration. This strategy allows an efficient nanoclay exfoliation in various matrices, e.g., starch and chitosan. Nevertheless, since this process is cost and time prohibitive, it may be not adapted for an industrial scale-up. Besides, the melt blending elaboration process appears as a better option to produce polysaccharide-based nano-biocomposites. However, plasticizer incorporation is often needed to melt the carbohydrate-based matrix and to limit its thermal degradation. According to the reported studies, these plasticizers greatly affect the nano-hybrid morphology with the establishment of strong hydrogen interactions with the nanofillers, which perturb the clay platelets intercalation/exfoliation process. Consequently, these nano-hybrids display mainly intercalated structures at high plasticizer content. To overcome this limitation and reach exfoliation, an organo-modification of the clay surface with hydrophilic surfactants, such as carbohydrate surfactants, has been proposed and tested to modify the nanofiller polarity and thus the clay/matrix affinity. Such nano-hybrid materials display improved mechanical reinforcement, higher thermal stability and barrier properties, and lower moisture sensitivity.

However, although a significant amount of work has already been performed on various aspects of polysaccharide nano-biocomposites, most researches still remain to understand the complex plasticizer/matrix/nanofiller interactions and their influence on the resulting morphology and materials properties. Indeed, it is known that high plasticizer content leads to inhomogeneous materials (e.g., plasticized starch with high glycerol content). Until now, no attention has been paid to the nanofiller influence on such phase separation and on the resulting nanostructuration. Thus, future investigations will have to include advanced characterization techniques to fully understand the complex interfacial behavior between the components of such multiphasic systems.

Besides, new nanocomposites have been recently elaborated from needle-shaped nanofillers (e.g., sepiolite, palygorskite, etc.) [209–211]. Compared to more conventional layered silicates, they present substantial differences, namely their aspect ratio and their surface properties (silanol groups located at the nanofiller surface) and thus could permit the elaboration of innovative polysaccharide-based nano-hybrid materials with extended properties.

To conclude, these polysaccharides/nanoclays materials are a valid answer to produce low cost, highly competitive and pioneering environmentally friendly materials. Moreover, since the citizens are more and more concerned about sustainable development and since the global need and the price of the fossil resources increase, such agro-based materials now represent an interesting option to replace conventional fossil resources based-plastics. Indeed, thanks to the agro-polymers intrinsic characteristics and improved properties brought by the nanofillers, these materials could present a wide range of applications, such as packaging, agriculture devices, or even for biomedical applications with some developments based on the biocompatibility of these materials.

References

[1] C.S.K. Reddy, R. Ghai, Rashmi, V.C. Kalia, Bioresour. Technol. 87 (2003) 137–146.
[2] R.G. Sinclair, J. Macromol. Sci. Part A-Pure Appl. Chem. 33 (1996) 585–597.
[3] R.A. Gross, B. Kalra, Science 297 (2002) 803–807.
[4] H. Tsuji, Y. Ikada, J. Appl. Polym. Sci. 67 (1998) 405–415.
[5] B. Cuq, N. Gontard, S. Guilbert, Cereal Chem. 75 (1998) 1–9.
[6] S. Guilbert, N. Gontard, L.G.M. Gorris, LWT-Food Sci. Technol. 29 (1996) 10–17.
[7] A. Redl, M.H. Morel, J. Bonicel, B. Vergnes, S. Guilbert, Cereal Chem. 76 (1999) 361–370.

[8] L. Averous, J. Macromol. Sci. Part C-Polym. Rev. 44 (2004) 231–274.
[9] M. Neus Angles, A. Dufresne, Macromolecules 33 (2000) 8344–8353.
[10] J.J.G. Van Soest, K. Benes, D. De Wit, J.F.G. Vliegenthart, Polymer 37 (1996) 3543–3552.
[11] K.J. Edgar, C.M. Buchanan, J.S. Debenham, P.A. Rundquist, B.D. Seiler, M.C. Shelton, D. Tindall, Prog. Polym. Sci. 26 (2001) 1605–1688.
[12] L. Averous, C. Fringant, Polym. Eng. Sci. 41 (2001) 727–734.
[13] L. Averous, L. Moro, P. Dole, C. Fringant, Polymer 41 (2000) 4157–4167.
[14] C.M. Buchanan, S.C. Gedon, A.W. White, M.D. Wood, Macromolecules 25 (1992) 7373–7381.
[15] A.A.S. Curvelo, A.J.F. De Carvalho, J.A.M. Agnelli, Carbohydr. Polym. 45 (2001) 183–188.
[16] A.K. Mohanty, M. Misra, L.T. Drzal, J. Polym. Environ. 10 (2002) 19–26.
[17] M. Wollerdorfer, H. Bader, Ind. Crop. Prod. 8 (1998) 105–112.
[18] L. Averous, N. Boquillon, Carbohydr. Polym. 56 (2004) 111–122.
[19] M. Alexandre, P. Dubois, Mater. Sci. Eng. R-Rep. 28 (2000) 1–63.
[20] S. Sinha Ray, M. Okamoto, Prog. Polym. Sci. 28 (2003) 1539–1641.
[21] R.A. Vaia, E.P. Giannelis, Macromolecules 30 (1997) 8000–8009.
[22] J.W. Cho, D.R. Paul, Polymer 42 (2001) 1083–1094.
[23] E.P. Giannelis, Adv. Mater. 8 (1996) 29–35.
[24] R. Krishnamoorti, R.A. Vaia, E.P. Giannelis, Chem. Mater. 8 (1996) 1728–1734.
[25] P.C. Lebaron, Z. Wang, T.J. Pinnavaia, Appl. Clay Sci. 15 (1999) 11–29.
[26] E.T. Thostenson, Z. Ren, T.W. Chou, Compos. Sci. Technol. 61 (2001) 1899–1912.
[27] O. Gain, E. Espuche, E. Pollet, M. Alexandre, P. Dubois, J. Polym. Sci. Pt. B-Polym. Phys. 43 (2005) 205–214.
[28] G. Gorrasi, M. Tortora, V. Vittoria, E. Pollet, M. Alexandre, P. Dubois, J. Polym. Sci. Pt. B-Polym. Phys. 42 (2004) 1466–1475.
[29] F. Chivrac, E. Pollet, L. Averous, J. Polym. Sci. Pt. B-Polym. Phys. 45 (2007) 1503–1510.
[30] E. Picard, J.F. Gerard, E. Espuche, J. Membr. Sci. 313 (2008) 284–295.
[31] E. Picard, A. Vermogen, J.F. Gerard, E. Espuche, J. Membr. Sci. 292 (2007) 133–144.
[32] T. Peprnicek, A. Kalendova, E. Pavlova, J. Simonik, J. Duchet, J.F. Gerard, Polym. Degrad. Stabil. 91 (2006) 3322–3329.
[33] F. Chivrac, Z. Kadlecova, E. Pollet, L. Averous, J. Polym. Environ. 14 (2006) 393–401.
[34] P.B. Messersmith, E.P. Giannelis, Chem. Mater. 5 (1993) 1064–1066.
[35] B. Lepoittevin, N. Pantoustier, M. Devalckenaere, M. Alexandre, D. Kubies, C. Calberg, R. Jerome, P. Dubois, Macromolecules 35 (2002) 8385–8390.
[36] G. Jimenez, N. Ogata, H. Kawai, T. Ogihara, J. Appl. Polym. Sci. 64 (1997) 2211–2220.
[37] B. Lepoittevin, M. Devalckenaere, N. Pantoustier, M. Alexandre, D. Kubies, C. Calberg, R. Jerome, P. Dubois, Polymer 43 (2002) 4017–4023.
[38] B. Lepoittevin, N. Pantoustier, M. Devalckenaere, M. Alexandre, C. Calberg, R. Jerome, C. Henrist, A. Rulmont, P. Dubois, Polymer 44 (2003) 2033–2040.
[39] M.A. Paul, M. Alexandre, P. Degee, C. Calberg, R. Jerome, P. Dubois, Macromol. Rapid Commun. 24 (2003) 561–566.
[40] M.A. Paul, C. Delcourt, M. Alexandre, P. Degee, F. Monteverde, A. Rulmont, P. Dubois, Macromol. Chem. Phys. 206 (2005) 484–498.
[41] N. Ogata, G. Jimenez, H. Kawai, T. Ogihara, J. Polym. Sci. Pt. B-Polym. Phys. 35 (1997) 389–396.
[42] M.A. Paul, M. Alexandre, P. Degee, C. Henrist, A. Rulmont, P. Dubois, Polymer 44 (2002) 443–450.
[43] M. Pluta, A. Galeski, M. Alexandre, M.A. Paul, P. Dubois, J. Appl. Polym. Sci. 86 (2002) 1497–1506.
[44] S. Sinha Ray, P. Maiti, M. Okamoto, K. Yamada, K. Ueda, Macromolecules 35 (2002) 3104–3110.
[45] P. Maiti, C.A. Batt, E.P. Giannelis, Biomacromolecules 8 (2007) 3393–3400.
[46] M.D. Sanchez-Garcia, E. Gimenez, J.M. Lagaron, J. Appl. Polym. Sci. 108 (2008) 2787–2801.
[47] P. Bordes, E. Pollet, S. Bourbigot, L. Averous, Macromol. Chem. Phys. 209 (2008) 1473–1484.
[48] S. Fischer, J. De Vlieger, T. Kock, L. Batenburg, H. Fischer, Materials Research Society Symposium—Proceedings, 2001, pp. 628–661.
[49] H.M. Park, X. Li, C.Z. Jin, C.Y. Park, W.J. Cho, C.S. Ha, Macromol. Mater. Eng. 287 (2002) 553–558.
[50] H.M. Park, W.K. Lee, C.Y. Park, W.J. Cho, C.S. Ha, J. Mater. Sci. 38 (2003) 909–915.
[51] B.S. Chiou, E. Yee, G.M. Glenn, W.J. Orts, D.F. Wood, S.H. Imam, ACS National Meeting Book of Abstracts, vol. 228, 2004.
[52] S.B. Hendricks, J. Geol. 50 (1942) 276–293.
[53] N. Jozja, Institut des sciences de la Terre (UMR 6313), Université d'Orléans, Orléans, 2003.
[54] F. Thomas, L.J. Michot, D. Vantelon, E. Montarges, B. Prelot, M. Cruchaudet, J.F. Delon, Colloid Surf. A-Physicochem. Eng. Asp. 159 (1999) 351–358.
[55] G. Sposito, D. Grasso, Surfactant Sci. Ser. 85 (1999) 107–249.
[56] J. Méring, Trans. Faraday Soc. 42B (1946) 205–219.
[57] P.F. Luckham, S. Rossi, Adv. Colloid Interface Sci. 82 (1999) 43–92.
[58] J.M. Cases, I. Brend, G. Besson, M. François, J.P. Uriot, F. Thomas, J.E. Poirier, Langmuir 8 (1992) 2730–2739.
[59] D.H. Powell, K. Tongkhao, S.J. Kennedy, P.G. Slade, Physica B 241–243 (1998) 387–389.
[60] D.H. Powell, H.E. Fischer, N.T. Skipper, J. Phys. Chem. B 102 (1998) 10899–10905.
[61] R. Tettenhorst, Am. Miner. 47 (1962) 769–773.
[62] J.C. Dai, J.T. Huang, Appl. Clay Sci. 15 (1999) 51–65.
[63] Y. Ke, J. Lü, X. Yi, J. Zhao, Z. Qi, J. Appl. Polym. Sci. 78 (2000) 808–815.
[64] G. Lagaly, Appl. Clay Sci. 15 (1999) 1–9.

[65] Z. Shen, G.P. Simon, Y.B. Cheng, Polymer 43 (2002) 4251–4260.
[66] H.R. Fischer, L.H. Gielgens, T.P.M. Koster, Acta Polym. 50 (1999) 122–126.
[67] C.A. Wilkie, J. Zhu, F. Uhl, Polym. Prepr. 42 (2001) 392.
[68] G. Lagaly, Solid State Ionics 22 (1986) 43–51.
[69] Y.H. Jin, H.J. Park, S.S. Im, S.Y. Kwak, S. Kwak, Macromol. Rapid Commun. 23 (2002) 135–140.
[70] H.R. Dennis, D.L. Hunter, D. Chang, S. Kim, J.L. White, J.W. Cho, D.R. Paul, Polymer 42 (2001) 9513–9522.
[71] A. Guilbot, C. Mercier, in: G.O. Aspinall (Ed.), Molecular Biology, vol. 3, Academic Press Incorporation, New York, 1985, pp. 209–282.
[72] G. Della Valle, A. Buleon, P.J. Carreau, P.A. Lavoie, B. Vergnes, J. Rheol. 42 (1998) 507–525.
[73] P. Colonna, C. Mercier, Carbohydr. Res. 126 (1984) 233–247.
[74] S. Hizukuri, Y. Takeda, M. Yasuda, Carbohydr. Res. 94 (1981) 205–213.
[75] A. Hayashi, K. Kinoshita, Y. Miyake, C.H. Cho, Polym. J. 13 (1981) 537–541.
[76] H.F. Zobel, Starch-Starke 40 (1988) 44–50.
[77] S. Hizukuri, Carbohydr. Res. 147 (1986) 342–347.
[78] P.J. Jenkins, A.M. Donald, Int. J. Biol. Macromol. 17 (1995) 315–321.
[79] J.J.G. Van Soest, S.H.D. Hulleman, D. De Wit, J.F.G. Vliegenthart, Ind. Crop. Prod. 5 (1996) 11–22.
[80] J.J.G. Van Soest, P. Essers, J. Macromol. Sci. Part A-Pure Appl. Chem. 34 (1997) 1665–1689.
[81] J.K. Jang, Y.R. Pyun, Starch-Starke 48 (1986) 48–51.
[82] R.L. Shogren, Carbohydr. Polym. 19 (1992) 83–90.
[83] C.L. Swanson, R.L. Shogren, G.F. Fanta, S.H. Imam, J. Environ. Polym. Degrad. 1 (1993) 155–166.
[84] I. Tomka, Adv. Exp. Med. Biol. 302 (1991) 627–637.
[85] D. Cooke, M.J. Gidley, Carbohydr. Res. 227 (1992) 103–112.
[86] D.J. Stevens, G.A.H. Elton, Starch-Starke 23 (1971) 8–11.
[87] N.K. Genkina, J. Wikman, E. Bertoft, V.P. Yuryev, Biomacromolecules 8 (2007) 2329–2335.
[88] A.L. Ollett, R. Parker, A.C. Smith, M.J. Miles, V.J. Morris, Carbohydr. Polym. 13 (1990) 69–84.
[89] O. Martin, L. Averous, G. Della Valle, Carbohydr. Polym. 53 (2003) 169–182.
[90] G. Della Valle, Y. Boche, P. Colonna, B. Vergnes, Carbohydr. Polym. 28 (1995) 255–264.
[91] B. Vergnes, J.P. Villemaire, P. Colonna, J. Tayeb, J. Cereal Sci. 5 (1987) 189.
[92] P.D. Orford, R. Parker, S.G. Ring, J. Cereal Sci. 18 (1993) 277–286.
[93] A.D. Sagar, E.W. Merrill, Polymer 36 (1995) 1883–1886.
[94] B. Baud, P. Colonna, G. Della Valle, P. Roger, in: P. Colonna, S. Guilbert (Eds.), Biopolymer Science: Food and Non Food Applications, Les Colloques de l'INRA, Paris, 1999, pp. 217–221.
[95] S.S. Wang, W.C. Chiang, A.I. Yeh, B. Zhao, I.H. Kim, J. Food Sci. 54 (1989) 1298–1301.
[96] V.J. Davidson, D. Paton, L.L. Diosady, G. Larocque, J. Food Sci. 49 (1984) 453–458.
[97] V.J. Davidson, R. Parker, L.L. Diosady, L.T. Rubin, J. Food Sci. 49 (1984) 1154–1169.
[98] K.J. Zeleznak, R.C. Hoseney, Cereal Chem. 64 (1987) 121–124.
[99] M.T. Kalichevsky, E.M. Jaroszkiewicz, S. Ablett, J.M.V. Blanshard, P.J. Lillford, Carbohydr. Polym. 18 (1992) 77–88.
[100] J.J.G. Van Soest, N. Knooren, J. Appl. Polym. Sci. 64 (1997) 1411–1422.
[101] P. Forssell, J. Mikkila, T. Suortti, J. Seppala, K. Poutanen, J. Macromol. Sci. Part A-Pure Appl. Chem. 33 (1996) 703–715.
[102] S.H.D. Hulleman, M.G. Kalisvaart, F.H.P. Janssen, H. Feil, J.F.G. Vliegenthart, Carbohydr. Polym. 39 (1999) 351–360.
[103] D. Lourdin, L. Coignard, H. Bizot, P. Colonna, Polymer 38 (1997) 5401–5406.
[104] J.J.G. Van Soest, D. De Wit, H. Tournois, J.F.G. Vliegenthart, Polymer 35 (1994) 4722–4727.
[105] S. Gaudin, D. Lourdin, P.M. Forssell, P. Colonna, Carbohydr. Polym. 43 (2000) 33–37.
[106] D. Lourdin, G. Della Valle, P. Colonna, Carbohydr. Polym. 27 (1995) 261–270.
[107] M.T. Kalichevsky, J.M.V. Blanshard, Carbohydr. Polym. 20 (1993) 107–113.
[108] A.L. Ollett, R. Parker, A.C. Smith, J. Mater. Sci. 26 (1991) 1351–1356.
[109] R.L. Shogren, C.L. Swanson, A.R. Thompson, Starch-Starke 44 (1992) 335–338.
[110] D. Lourdin, S.G. Ring, P. Colonna, Carbohydr. Res. 306 (1998) 551–558.
[111] D. Lourdin, H. Bizot, P. Colonna, Macromol. Symp. 114 (1997) 179–185.
[112] D. Lourdin, H. Bizot, P. Colonna, J. Appl. Polym. Sci. 63 (1997) 1047–1053.
[113] L. Godbillot, P. Dole, C. Joly, B. Roge, M. Mathlouthi, Food Chem. 96 (2006) 380–386.
[114] H.J. Thiewes, P.A.M. Steeneken, Carbohydr. Polym. 32 (1997) 123–130.
[115] T.J. Lu, J.L. Jane, P.L. Keeling, Carbohydr. Polym. 33 (1997) 19–26.
[116] I.A.M. Appelqvist, D. Cooke, M.J. Gidley, S.J. Lane, Carbohydr. Polym. 20 (1993) 291–299.
[117] L. Averous, N. Fauconnier, L. Moro, C. Fringant, J. Appl. Polym. Sci. 76 (2000) 1117–1128.
[118] J.J.G. Van Soest, D.B. Borger, J. Appl. Polym. Sci. 64 (1997) 631–644.
[119] J.J.G. Van Soest, D. De Wit, J.F.G. Vliegenthart, J. Appl. Polym. Sci. 61 (1996) 1927–1937.
[120] J.J.G. Van Soest, S.H.D. Hulleman, D. De Wit, J.F.G. Vliegenthart, Carbohydr. Polym. 29 (1996) 225–232.
[121] H.-M. Wilhelm, M.-R. Sierakowski, G.P. Souza, F. Wypych, Polym. Int. 52 (2003) 1035–1044.
[122] P. Kampeerapappun, D. Aht-ong, D. Pentrakoon, K. Srikulkit, Carbohydr. Polym. 67 (2007) 155–163.
[123] B.-S. Chiou, E. Yee, G.M. Glenn, W.J. Orts, Carbohydr. Polym. 59 (2005) 467–475.
[124] B. Chen, J.R.G. Evans, Carbohydr. Polym. 61 (2005) 455–463.
[125] Q.X. Zhang, Z.Z. Yu, X.L. Xie, K. Naito, Y. Kagawa, Polymer 48 (2007) 7193–7200.

[126] B.-S. Chiou, E. Yee, D. Wood, J. Shey, G. Glenn, W. Orts, Cereal Chem. 83 (2006) 300–305.
[127] M. Avella, J.J. De Vlieger, M.E. Errico, S. Fischer, P. Vacca, M.G. Volpe, Food Chem. 93 (2005) 467–474.
[128] M. Chen, B. Chen, J.R.G. Evans, Nanotechnology 16 (2005) 2334–2337.
[129] B.S. Chiou, D. Wood, E. Yee, S.H. Imam, G.M. Glenn, W.J. Orts, Polym. Eng. Sci. 47 (2007) 1898–1904.
[130] M.F. Huang, J.G. Yu, X.F. Ma, Polymer 45 (2004) 7017–7023.
[131] J.K. Pandey, R.P. Singh, Starch-Starke 57 (2005) 8–15.
[132] V.P. Cyras, L.B. Manfredi, M.T. Ton-That, A. Vazquez, Carbohydr. Polym. 73 (2008) 55–63.
[133] X. Ma, J. Yu, N. Wang, Macromol. Mater. Eng. 292 (2007) 723–728.
[134] K. Dean, L. Yu, D.Y. Wu, Compos. Sci. Technol. 67 (2007) 413–421.
[135] M. Huang, J. Yu, J. Appl. Polym. Sci. 99 (2006) 170–176.
[136] M. Huang, J. Yu, X. Ma, Acta Polym. Sin. (2005) 862–867.
[137] M. Huang, J. Yu, X. Ma, Carbohydr. Polym. 63 (2006) 393–399.
[138] M.F. Huang, J.G. Yu, X.F. Ma, Chin. Chem. Lett. 16 (2005) 561–564.
[139] M.F. Huang, J.G. Yu, X.F. Ma, P. Jin, Polymer 46 (2005) 3157–3162.
[140] K. Bagdi, P. Muller, B. Pukanszky, Compos. Interfaces 13 (2006) 1–17.
[141] X. Tang, S. Alavi, T.J. Herald, Cereal Chem. 85 (2008) 433–439.
[142] X. Tang, S. Alavi, T.J. Herald, Carbohydr. Polym. 74 (2008) 552–558.
[143] D.S. Chaudhary, J. Polym. Sci. Pt. B-Polym. Phys. 46 (2008) 979–987.
[144] N. Lilichenko, R.D. Maksimov, J. Zicans, R. Merijs Meri, E. Plume, Mech. Compos. Mater. 44 (2008) 45–56.
[145] M. Mondragon, J.E. Mancilla, F.J. Rodriguez-Gonzalez, Polym. Eng. Sci. 48 (2008) 1261–1267.
[146] K.M. Dean, M.D. Do, E. Petinakis, L. Yu, Compos. Sci. Technol. 68 (2008) 1453–1462.
[147] F. Chivrac, E. Pollet, M. Schmutz, L. Averous, Biomacromolecules 9 (2008) 896–900.
[148] S.Y. Lee, Y.X. Xu, M.A. Hanna, Int. Polym. Process 22 (2007) 429–435.
[149] S.Y. Lee, M.A. Hanna, J. Appl. Polym. Sci. 110 (2008) 2337–2344.
[150] S.Y. Lee, M.A. Hanna, D.D. Jones, Starch/Staerke 60 (2008) 159–164.
[151] S.Y. Lee, H. Chen, M.A. Hanna, Ind. Crop. Prod. 28 (2008) 95–106.
[152] C.J. Perez, V.A. Alvarez, I. Mondragon, A. Vazquez, Polym. Int. 56 (2007) 686–693.
[153] C.J. Perez, V.A. Alvarez, P.M. Stefani, A. Vazquez, J. Therm. Anal. Calorim. 88 (2007) 825–832.
[154] C.J. Perez, V.A. Alvarez, I. Mondragon, A. Vazquez, Polym. Int. 57 (2008) 247–253.
[155] C.J. Perez, A. Vazquez, V.A. Alvarez, J. Therm. Anal. Calorim. 91 (2008) 749–757.
[156] C.J. Perez, V.A. Alvarez, A. Vazquez, Mater. Sci. Eng. A-Struct. 480 (2008) 259–265.
[157] S.A. McGlashan, P.J. Halley, Polym. Int. 52 (2003) 1767–1773.
[158] S.B. Kalambur, S.S. Rizvi, Polym. Int. 53 (2004) 1413–1416.
[159] S. Kalambur, S.S.H. Rizvi, J. Appl. Polym. Sci. 96 (2005) 1072–1082.
[160] X. Qiao, W. Jiang, K. Sun, Starch-Starke 57 (2005) 581–586.
[161] Y. Xu, J. Zhou, M.A. Hanna, Cereal Chem. 82 (2005) 105–110.
[162] N.V. Pogodina, C. Cerclé, L. Averous, R. Thomann, M. Bouquey, R. Muller, Rheol. Acta 47 (2008) 543–553.
[163] F. Chivrac, O. Gueguen, E. Pollet, S. Ahzi, A. Makradi, L. Averous, Acta Biomater. 4 (2008) 1707–1714.
[164] O. Martin, L. Averous, Polymer 42 (2001) 6209–6219.
[165] P. Maiti, K. Yamada, M. Okamoto, K. Ueda, K. Okamoto, Chem. Mater. 14 (2002) 4654–4661.
[166] C. Fringant, J. Desbrieres, M. Rinaudo, Polymer 37 (1996) 2663–2673.
[167] H.-M. Wilhelm, M.-R. Sierakowski, G.P. Souza, F. Wypych, Carbohydr. Polym. 52 (2003) 101–110.
[168] H. Lilholt, J.M. Lawther, in: A. Kelly, C. Zweben (Eds.), Comprehensive Composite Materials, vol. 1, Elsevier, 2000, pp. 303–325.
[169] R.H. Atalla, D.L. Van der Hart, Science 223 (1984) 283–285.
[170] D.L. Van der Hart, R.H. Atalla, Macromolecules 17 (1984) 1465–1472.
[171] A.P. Heiner, O. Teleman, Langmuir 13 (1997) 511–518.
[172] Y. Nishiyama, P. Langan, H. Chanzy, J. Am. Chem. Soc. 124 (2002) 9074–9082.
[173] H. Chanzy, in: J.F. Kennedy, G.O. Phillips, P.A. Williams (Eds.), Cellulose Sources and Exploitation, Ellis Horwood Ltd., New York, 1990, pp. 3–12.
[174] J.F. Revol, J. Mater. Sci. Lett. 4 (1985) 1347–1349.
[175] L. Sakurada, Y. Nukushina, T. Ito, J. Polym. Sci. 57 (1962) 651–660.
[176] A. Dufresne, M.R. Vignon, Macromolecules 31 (1998) 2693–2696.
[177] M.E. Gomes, A.S. Ribeiro, P.B. Malafaya, R.L. Reis, A.M. Cunha, Biomaterials 22 (2001) 883–889.
[178] H.M. Park, M. Misra, L.T. Drzal, A.K. Mohanty, Biomacromolecules 5 (2004) 2281–2288.
[179] A.C. Wibowo, M. Misra, H.M. Park, L.T. Drzal, R. Schalek, A.K. Mohanty, Compos. Pt. A-Appl. Sci. Manuf. 37 (2006) 1428–1433.
[180] H.M. Park, X. Liang, A.K. Mohanty, M. Misra, L.T. Drzal, Macromolecules 37 (2004) 9076–9082.
[181] H.M. Park, A.K. Mohanty, L.T. Drzal, E. Lee, D.F. Mielewski, M. Misra, J. Polym. Environ. 14 (2006) 27–35.
[182] M. Yoshioka, K. Takabe, J. Sugiyama, Y. Nishio, J. Wood Sci. 52 (2006) 121–127.
[183] G. Gorrasi, M. Tortora, V. Vittoria, E. Pollet, B. Lepoittevin, M. Alexandre, P. Dubois, Polymer 44 (2003) 2271–2279.
[184] N.A. Campbell, J.B. Reece, L.G. Mitchell, Biology, Menlo Park CA, New Work, 1999
[185] M. Rinaudo, Prog. Polym. Sci. 31 (2006) 603–632.
[186] K.M. Rudall, W. Kenchington, Biol. Rev. 40 (1973) 597–636.
[187] E.D.T. Atkins, J. Biosci. 8 (1985) 375–387.
[188] R. Minke, J. Blackwell, J. Mol. Biol. 120 (1978) 167–181.
[189] K.H. Gardner, J. Blackwell, Biopolymers 14 (1975) 1581–1595.
[190] Y. Lu, L. Weng, L. Zhang, Biomacromolecules 5 (2004) 1046–1051.
[191] M. Paillet, A. Dufresne, Macromolecules 34 (2001) 6527–6530.
[192] M.G.P.I. Peter, in: A. Steinbüchel (Ed.), Biopolymers, Vol. 6: Polysaccharides II, Wiley-VCH, Weinheim, 2002, pp. 123–157.
[193] F. Shahidi, J.K.V. Arachchi, Y.J. Jeon, Trends Food Sci. Technol. 10 (1999) 37–51.
[194] K. Ogawa, Agric. Biol. Chem. 55 (1991) 2375–2379.
[195] K. Ogawa, T. Yui, M. Miya, Biosci. Biotech. Biochem. 56 (1992) 858–862.
[196] M. Darder, M. Colilla, E. Ruiz-Hitzky, Chem. Mater. 15 (2003) 3774–3780.
[197] Y. Xu, X. Ren, M.A. Hanna, J. Appl. Polym. Sci. 99 (2006) 1684–1691.
[198] E. Günister, D. Pestreli, C.H. Unlu, O. Atici, N. Gungor, Carbohydr. Polym. 67 (2007) 358–365.
[199] M. Darder, M. Colilla, E. Ruiz-Hitzky, Appl. Clay Sci. 28 (2005) 199–208.
[200] S. Wang, L. Chen, Y. Tong, J. Polym. Sci. Pt. A-Polym. Chem. 44 (2006) 686–696.
[201] S.F. Wang, L. Shen, Y.J. Tong, L. Chen, I.Y. Phang, P.Q. Lim, T.X. Liu, Polym. Degrad. Stabil. 90 (2005) 123–131.
[202] X. Wang, Y. Du, J. Yang, W.X., X. Shi, Y. Hu, Polymer 47 (2006) 6738–6744.
[203] K.-F. Lin, C.-Y. Hsu, T.-S. Huang, W.-Y. Chiu, Y.-H. Lee, T.-H. Young, J. Appl. Polym. Sci. 98 (2005) 2042–2047.
[204] J.J. Luo, I.M. Daniel, Compos. Sci. Technol. 63 (2003) 1607–1616.
[205] B.R. Thakur, R.K. Singh, A.K. Handa, Crit. Rev. Food Sci. Nutr. 37 (1997) 47–73.
[206] C.D. May, Carbohydr. Polym. 12 (1990) 79–99.
[207] P. Mangiacapra, G. Gorrasi, A. Sorrentino, V. Vittoria, Carbohydr. Polym. 64 (2006) 516–523.
[208] M. Magini, C. Colella, A. Iasonna, F. Padella, Acta Mater. 46 (1998) 2841–2850.
[209] E. Bilotti, H.R. Fischer, T. Peijs, J. Appl. Polym. Sci. 107 (2008) 1116–1123.
[210] L. Bokobza, A. Burr, G. Garnaud, M.Y. Perrin, S. Pagnotta, Polym. Int. 53 (2004) 1060–1065.
[211] E. Duquesne, S. Moins, M. Alexandre, P. Dubois, Macromol. Chem. Phys. 208 (2007) 2542–2550.
[212] A.K. Bledzki, J. Gassan, Prog. Polym. Sci. 24 (1999) 221–274.